Artificial lake induced seismicity – a summary

Shell Global Solutions, October 2015

This note summarizes a two-week literature search on the current knowledge of reservoir (artificial lake) induced seismicity (RIS). The seismicity caused by impounding in hydro-electricity water reservoirs may possibly provide NAM with insights into the relation between induced seismicity across the Groningen gas field and production fluctuations. To optimize time spent on the literature search this report is delivered in note-form, with parts of the texts of the referenced publications incorporated without major modifications.

1 Introduction

Reservoir induced seismicity (RIS) is defined as the failure of a pre-existing fault below an artificial lake due to reservoir impoundment after initial infill or by seasonal water level fluctuations. Up to 2012, there have been 127 RIS cases reported around the world. Among them, 4 cases of strong earthquakes (M≥6), 15 cases of moderate earthquakes (5.9≥M≥5) and 32 cases of light earthquakes (4.9≥M≥4) can be found (Qiu, 2012). Case investigations indicate that strong correlations exist between the occurrence of induced seismicity and reservoir size and filling history, hydrogeological conditions, faulting regime, and rock types.

In this note, the main findings from two RSI summaries and 15 case related papers or studies/experiments across the globe are bundled. After discussing the earlier mentioned main factors, that induce seismicity in artificial lakes (section 2), RSI patterns are presented (section 3) and laboratory tests on well cores and a borehole experiment on an normal fault used to describe the mechanisms, pore pressure diffusion and mechanical property variations in the subsurface, that control the size and style of reservoir induced seismicity (section 4).

2 Global observations

2.1 Reservoir size

Table 1 shows that there is a very strong positive correlation between increasing reservoir size (dam height and capacity) and increased probability of RIS occurrence. However, reservoir size is neither a necessary nor a sufficient condition for RIS to occur since RIS cases also occur in small-size reservoirs (capacity $\leq$1km^3) and some large-size reservoirs (capacity $\geq$10 km^3) do not trigger any seismicity at all (Qiu, 2012).

Dam height (m)	Number of reservoirs	Number of RIS cases	Likelihood of RIS
≤50	33083	15	0.05%
50~100	3537	33	0.93%
100~150	573	37	6.46%
>150	187	32	17.11%

Table 1: Dam height and likelihood of RIS

2.2 Faulting regime

The majority of the RIS cases are caused by the reactivation of existing discontinuities rather than the development of new faults. The column of water in an artificial lake alters the in-situ stress along an existing fault and its weight can significantly change the stress on an underlying fault by increasing the total stress through direct loading, or decreasing the effective stress through the increased pore water pressure. RIS sites very often coincide with critical locations, which are very close to failure. Small stress increases of less than 0.05 MPa are assumed to be enough to trigger earthquakes.

Among the 127 RIS reservoir sites evaluated by Qui (2012), 79% are located in normal or strike-slip faulting environments, while only 21% are in reverse faulting environments (Figure 1). The phenomenon that reservoirs located in reverse faulting regimes are less susceptible to RIS than reservoirs in normal or strike-slip faulting regimes can be explained by constructing a simple Mohr- Coulomb failure model. In an environment of reverse faulting, the minimum principal stress is in the vertical direction. Reservoir impoundment will directly increase the minimum principal stress, thus decreasing the diameter of Mohr circle, moving it further away from the failure envelope.

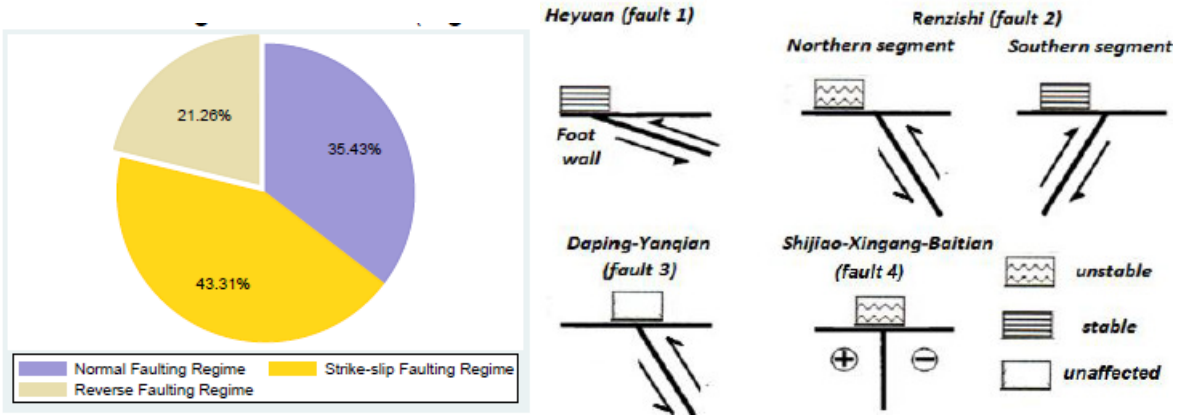

Figure 1: On the left the tectonic setting (types of faulting) for 127 worldwide RIS cases and on the right the effects of oscillating reservoir loads. The location of the fault relative to the reservoir determines whether the oscillating reservoir loads have a stabilising or destabilising effect (seismicity) on the fault (modified by many after Roeloffs, 1988).

Faults are considered as structurally anisotropic and lithologically heterogeneous. In terms of permeability, they can either assist or impede water flow depending on their permeability structures (do Nascimento, 2005). Fractures in fault zones that have their permeability within the seismogenic permeability range (0.5 – 50mD) can allow pore water to diffuse as Darcian flow, thus making it easier to induce seismicity (Figure 2). However if the fracture permeability is lower than the seismogenic permeability, then the flow through the fracture is negligible, causing only a small pore pressure increases. If the fracture permeability is higher than the seismogenic permeability, then the flow rate is too large to act as a Darcian flow, and pore pressure diffusion is unlikely to occur (Talwani, 2007, Qui, 2012).

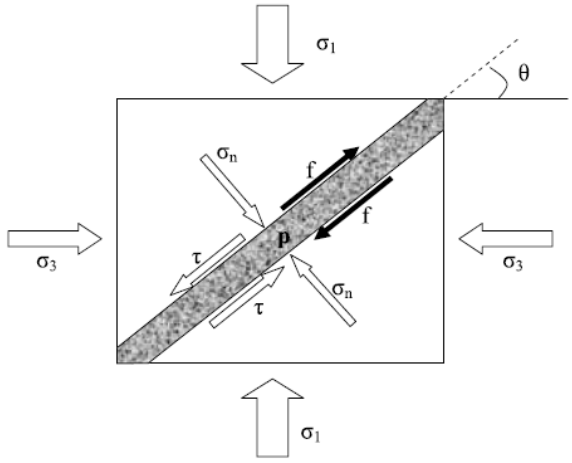

Figure 2: A fluid-filled fracture with pore fluid pressure p subjected to a two-dimensional stress field. Ϭn, t, and f are the normal, shear, and frictional stresses, respectively.

2.3 Rock Types

The investigations of cases where RSI has occurred also showed that reservoir areas underlain by carbonate or crystalline rocks are most likely to experience induced seismicity (Figure 3). Carbonate rocks are the most vulnerable rock type to chemical dissolution, which reduces cohesion and coefficient of friction, thus weakening the fault strength. The dissolved material may also be washed away by the un-drained water flow, resulting in the widening of fractures, weakening of rock strength and increase in fracture permeability. Most crystalline rocks, especially granite, can't be treated as an equivalent porous medium. In a large granite body, more than 80% of the water flow is contained in several major pre-existing fractures. The reservoir impoundment will increase this water flow, saturation and pore pressure in the fractures of granites and hence, make these fractures often critically stressed and on the threshold of failure (Qui, 2012).

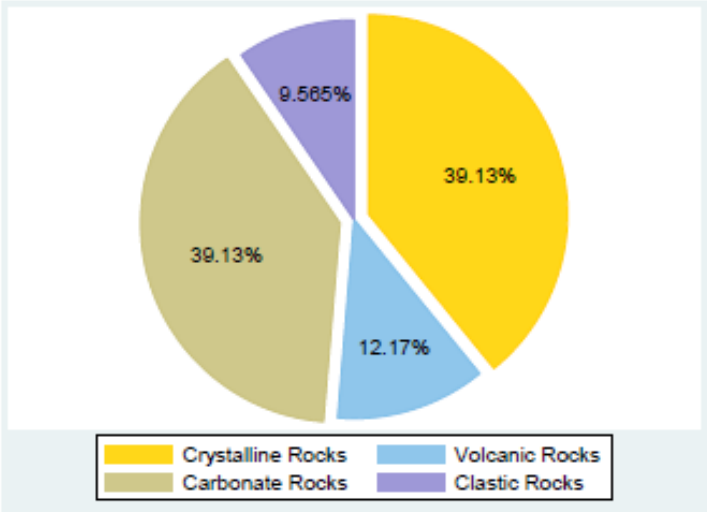

Figure 3: Rock types in reservoir regions experiencing RIS (115 cases worldwide).

2.4 Reservoir Filling History

The Lake Mead reservoir in the USA and Koyna reservoir in India (Kumar, 2012) provide nice examples to demonstrate the impact of the reservoir filling history on induced seismicity with major activity increases occurring soon after the water level reached a new or approached a previous maximum (Figures 4 and 5).

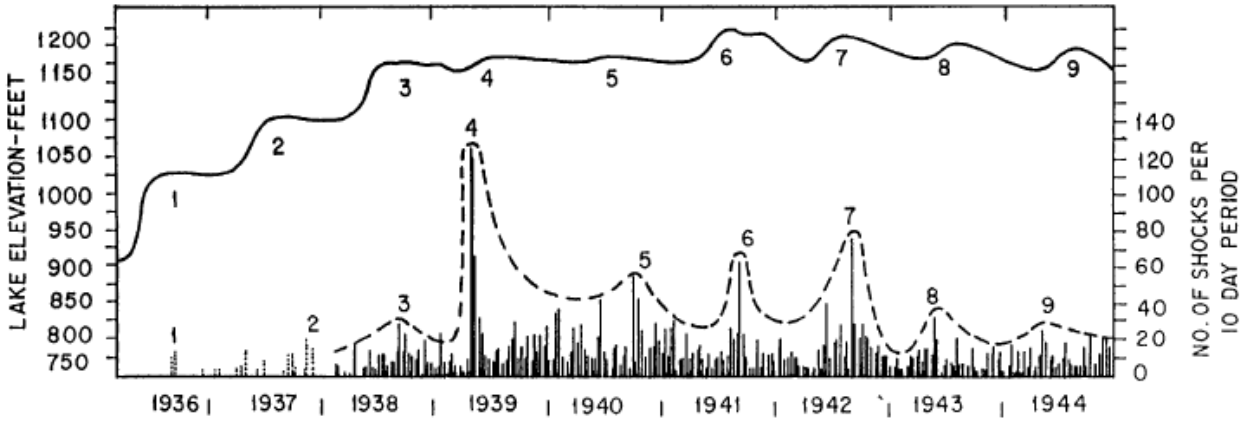

Figure 4: The rises in water levels in Lake Mead and the corresponding bursts of seismic activity are numbered. General trend of tremor-frequency variation is shown by dotted lines. **Note**: author believes that the delay between fill and event shortens over time and that burst 4 most likely results from fill 3.

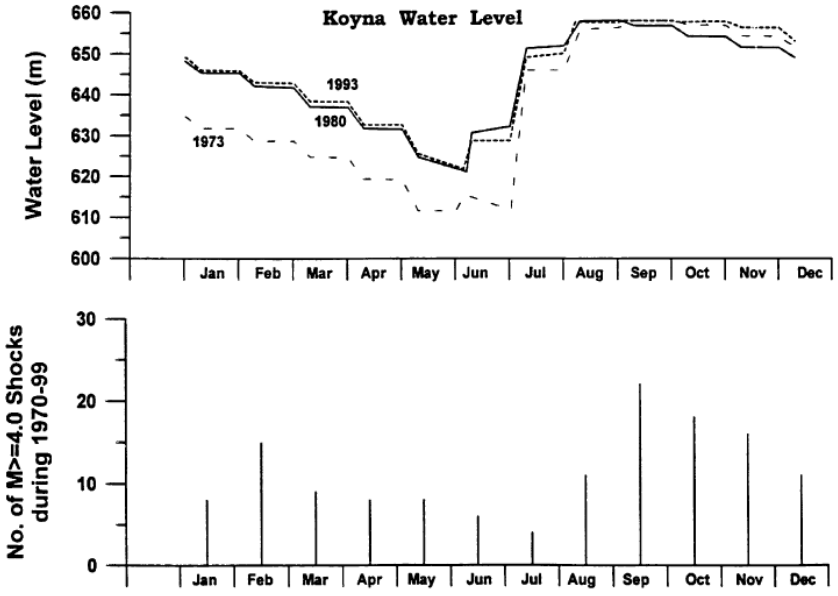

Figure 5: Water levels in Koyna reservoir for the years 1973, 1980 and 1993 and the monthly number of earthquakes of M 4 and larger for the period 1970 through 1999. The Koyna reservoir is underlain by a strongly faulted subsurface. Any change in loading in the Koyna reservoir results directly in an increase in RSI (Kumar, 2012).

3 RSI patterns

Figures 4 and 5 also show that RSI often comes in shock patterns consisting of small foreshocks, a big main shock and smaller again aftershocks. Mogi's (1963) has related these patterns to the structures of materials and applied stresses and classified them into three types (Figure 6):

- **Type I**: in the case of homogeneous material and uniformly applied stress, a main shock occurs without any foreshock and is followed by numerous elastic aftershocks.
- **Type II**: when the material has a rather heterogeneous structure and/or the applied stress is not uniform, small elastic shocks occur prior to a main shock and many aftershocks occur following the main shock.
- **Type III**: when the structure of the material is extremely heterogeneous and/or the applied stress has a considerable concentration, a swarm type of activity occurs consisting of a number of elastic shocks with magnitudes increase gradually and then decrease after some time.

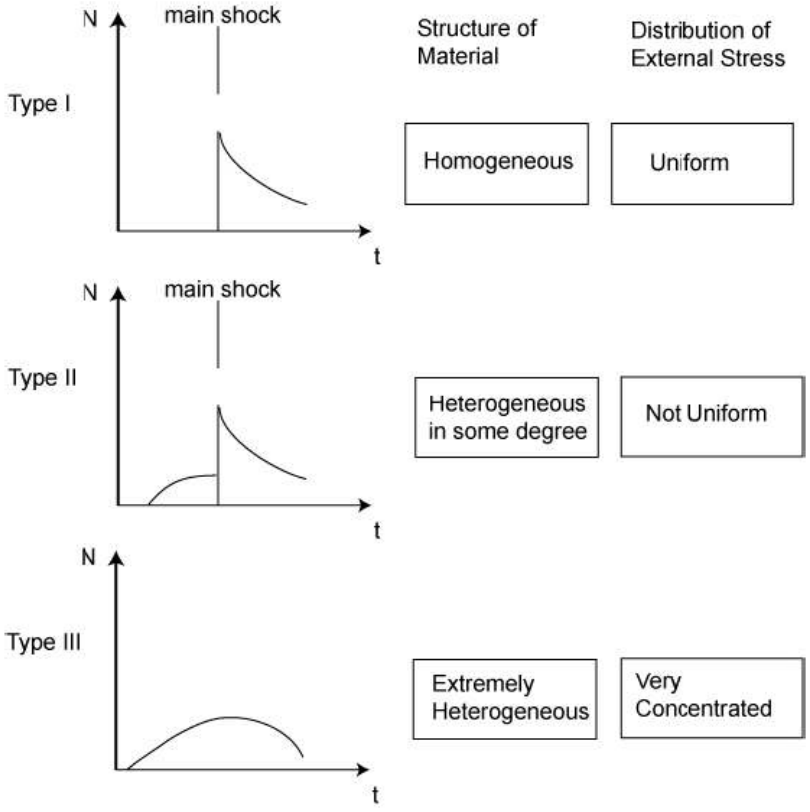

Figure 6: Induced seismicity patterns from Mogi (1963) based on the structure of materials below an artificial lake and applied stresses due to the impoundment (N is the number of seismic events and t is the time).

The above seismicity patterns have been divided by Talwani (1997), Chen and Talwani (2001) and Ying (2012) into temporal categories to describe time delays between artificial lake impoundment and event and style of the seismic event (see text next page):

- **Rapid and delayed seismic responses**

Rapid responses follow immediately after the initial loading of the reservoir or after a rapid change in reservoir water level. They consist primarily of low magnitude, swarm-like activity that are confined to the immediate reservoir area and caused by changes in elastic stress or a pore-pressure change coupled to the elastic stress. Pore pressure diffusion is not a major factor for inducing rapid seismicity.

Delayed responses come with relatively larger earthquakes which suggest that seismicity has extended significantly beyond the confines of the reservoir. It is generally accepted that diffusion of pore pressure is the mechanism responsible for these spatial and temporal effects of RIS. Depending on the permeability and the fracture network in the rock, it may take months or years for the pore pressure effect to spread into the subsurface. When the pore pressure pulse finally reaches a zone of micro-cracks, it may force water into the cracks and reduce the normal stress that holds the strained faults, consequently triggering delayed (depending on permeability of the rocks involved) seismicity.

- **Initial and protracted seismicity**

Initial seismicity is associated with initial reservoir impoundment or a large water level change. This applies to seismicity associated with water level increases above the previous attained maximum. It results from the almost instantaneous effect of loading, as well as the delayed effect of pore pressure diffusion. The delay between the start of impoundment and the increase in frequency and magnitude of seismicity varies from months to years and is associated with the reservoir characteristics, local geology, and mechanical conditions of the rocks involved. The initial increase in the frequency and magnitude of earthquakes will reduce progressively, indicating the cessation of the coupled poro-elastic response to the impoundment as the rocks involved slowly adjust to the added weight by extra compaction.

Protracted seismicity occurs after the effect of initial filling of the reservoir has diminished. It is often associated with the frequency and amplitude of water level changes, particularly with lower frequencies (longer periods). This seismicity is observed both beneath the deepest part of the reservoir and in the surrounding areas. This seismicity can persist for many years without decrease in frequency and magnitude.

4 Understanding the mechanisms that cause RSI via experiments

4.1 Laboratory experiments on cores

Tri-axial experiments have been conducted by Ying (2010) on low porosity (~4%) / low permeability (=more indurated) and high porosity (~13%) / high permeability (= less quartz-cemented) sandstone well cores (both containing >98% quartz) to investigate the effects of oscillating pore pressure on induced seismicity (Figure 7). Geophysical techniques were used to reconstruct and analyse the spatial and temporal distribution of seismic events. Cyclic pore pressures were applied to the naturally-fractured samples to activate and reactivate the existing faults. Their results indicate that the mechanical properties of the rocks involved and the heterogeneity of the fault zone can influence the seismic response.

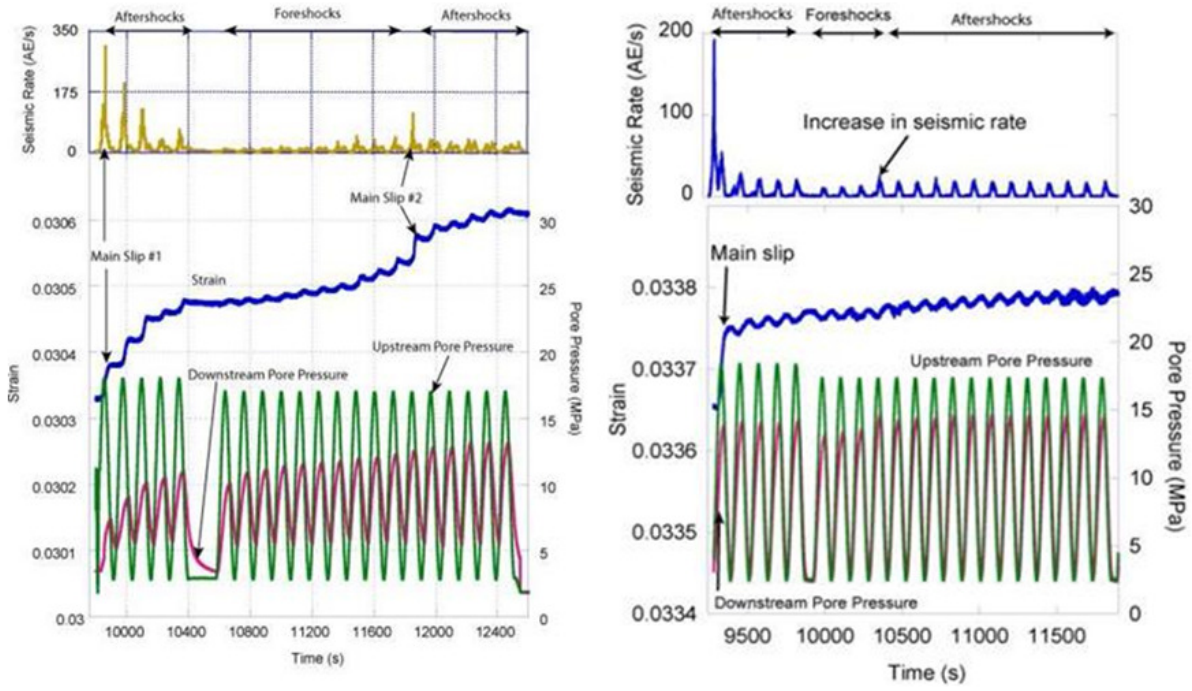

Figure 7: Two of the experiments, on the left with a step-wise (step 1 and 2) increase and on the right with oscillating/cyclic pore pressure (middle blue line for both). In the step increase experiment on the left, the first 5 cycles simulate an aftershock sequence in which pore pressure was oscillated sinusoidally between 18 and 2.5 MPa, with a period of 2 minutes. The subsequent 16 cycles simulate a foreshock-main shock-aftershock sequence, when pore pressure was oscillated between 17 and 2.5 MPa. Fault reactivation intensified after the 6th cycle, when the change in strain increased and the main slip 2 occurred at the 11th cycle. In the oscillating experiment on the right, the seismic rate developed slightly in the first 4 cycles of the foreshock sequence; however, due to the limited increase in downstream pore pressure, the corresponding strain did not change significantly. Upstream and downstream refer to top (read lake bottom) and bottom of the core samples.

In the experiments, initial seismicity was induced by applying pore pressures that exceeded the previous attained maximum pore pressure. Fault reactivations and foreshock sequences were found in the low permeable sandstone experiments. With the seismic rate histories

indicating that oscillating pore pressure can induce seismicity for a longer time period than a single-step increase in pore pressure. The corresponding strain change due to cyclic pore pressure changes suggests that progressive shearing occurred during the pore pressure cycles. This shearing progressively damaged the existing fault through the abrasion of asperities (points of resistance), which in turn reduced the friction coefficient and, hence, reduced the shear strength of the fault. This 'slow' seismic mechanism increasingly hindered the diffusion of the pore pressure and contributed to the prolonged period of seismicity.

The following points summarize the main findings of Ying's laboratory experiments:

- **Pore pressure variation** can induce initial seismicity as well as protracted seismicity as the average pore pressure within the system may continue to increase during the cycles despite the lowered oscillation pore pressure peaks immediately below the reservoir. This phenomenon may be explained by **the Kaiser effect**, which describes that if a material is experiencing cyclic loading with increasing stress, there is an increase in micro seismicity (in the form of acoustic emission) if the highest stress level of the previous loading cycle (maximum water level) is exceeded.

- The **mechanical properties of material**, **frequency of oscillation** and **rate of increase of pore pressure** influence the growth of seismicity and control the amount and size of the protracted RIS.

- **Mechanical rock properties** can influence the reactivation of a fault and induce protracted seismicity. The factors that affect the protracted seismic response include:
  i) The interconnected porosity and permeability of the fractured sample. When porosity and permeability are low then the pore pressure will stay at a transient state for a long period of time
  ii) The heterogeneity of the fractured sample also influences the development of the foreshock sequence. In case pore pressures diffuse easily no foreshocks are found in homogeneous media, but precede the main shock in slightly heterogeneous media

- **Oscillating (e.g., annually) pore pressure**, compared to a stepped increase in pore pressure, can tighten the rock by inducing progressive shearing, which may slow down the pore pressure (diffusion) development in the system and extend the period of seismicity. This progressive shearing can gradually smooth the asperities at the fractured contact surface and reduce the friction coefficient, consequently reducing the shear strength of the fault and causing protracted failures.

- If the **rate of pore pressure increase** during initial reservoir impoundment can be controlled at a slower rate (for instance spread out over a decade), then induced seismicity is less likely to occur as the subsurface will get more time to adjust to the extra weight added by the water resevoir.

4.2 Borehole injection experiment in a shallow normal fault

In this borehole injection experiment slow slip reactivation was nucleated at 280m depth through the artificial pressurization of a 10m long segment of a normal fault while continuously monitoring strain, seismicity and pore pressures (Guglielmi, 2013). The experiment highlights the importance of the fluid influence in fault failure,

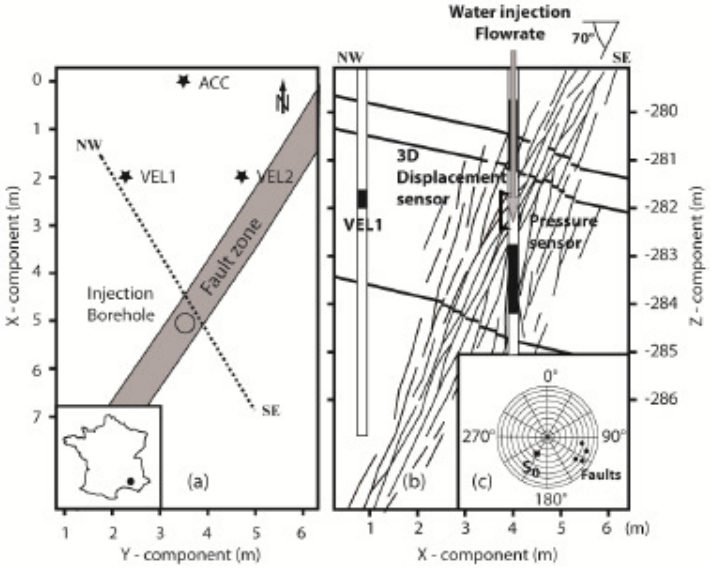

Figure 8: (a) Map view of the injected fault zone and observation holes, (b) Vertical cross section with the injection and monitoring devices set across the fault and (c) Stereographic projection of the main fracture planes (upper hemisphere, S0 is bedding plane pole).

The fault in this experiment has a meter scale offset and intersects limestone layers characterized by a porosity of 4 to 10%, a permeability of 1 to 4×10-13m^2, and a Bulk modulus of 30 to 40 GPa. The fault zone is 2m thick with sub-parallel pre-existing connected fractures of metric scale (Figure 8). Discontinuous thin breccia's zones are observed close to some fracture planes. The fault zone has an average permeability of 10-12m^2 and a bulk modulus of 10 to 17 GPa that are a factor 25 higher and a factor 2-to-5 lower than the surrounding country rock, respectively. Pressure sensors were located in a 1.5m long chamber that was isolated between two inflatable packers.

This field experiment has identified **three successive steps** for the fluid influence in fault failure, which are stress, strain and permeability (flowrate) dependent (Figure 9).

- In the **first** phase, fault instability by frictional weakening is triggered by an increased fluid pressure. This abrasive rock cutting in the fault zone leads to an increase in permeability (K).

- In the **second** phase, this higher K permits fluid diffusion to spread which results in a slight decrease in effective normal stress. During this period, fault failure is strain dependent, driven by two competing mechanisms, the effective normal stress variation with fluid diffusion time and many slow small-radiated-energy ruptures

(tremors) occurring on a larger fault zone than the little ones where the fluid injection takes place.

- In the **third** phase, permeability in the new large fault zone gradually increases while the friction coefficient remains low. During this period, fault failure is controlled by the fault permeability and porosity variations in a large active shear zone. That porosity is increasing in this phase of the experiment is illustrated by the numerous transient pressure drops observed during this period. The high dilation rate favors a drained fault behavior characterized by a stable low-to-aseismic slip regime. The increase in permeability, which is deduced from numerical analysis (Figure 10, lower graph), shows that connection between the pores occurs very fast within the large failure plane.

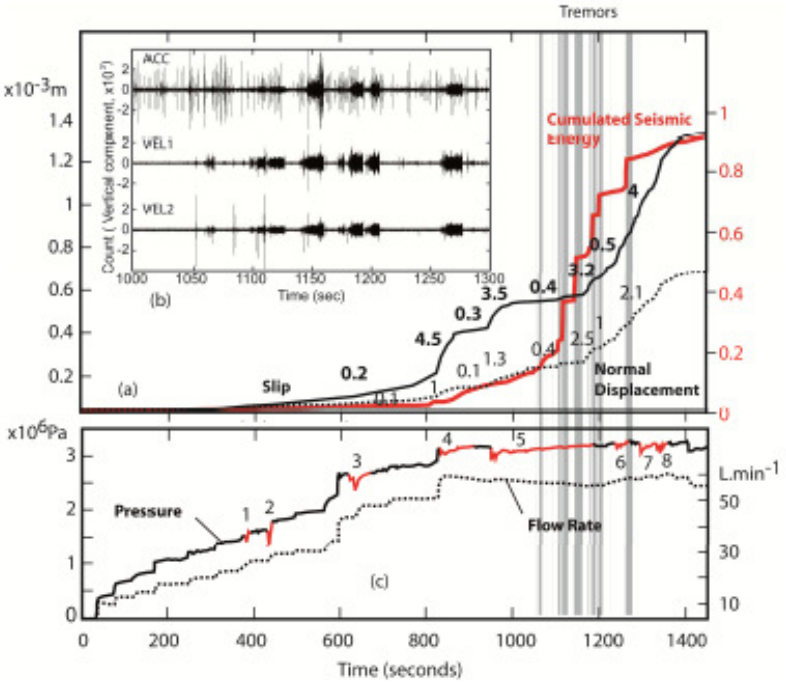

Figure 9: (a) In situ monitoring of fault slip, normal displacement and cumulated seismic energy (values 0.2-to-4.5 (bold black numbers) and 0.1-to- 2.5 (black numbers next to dashed line) respectively correspond to slip velocities and dilatant rate expressed in micrometers per seconds), (b) Zoom of the Y component accelerometer signal recorded at location ACC (see figure 8) in the 1000 to 1400 seconds time interval. This component was chosen because of the high energy radiated by the tremor shear waves in that direction. This curve displays an example of the different seismo-acoustic events recorded during the experiment, (c) Pressure and injected flow rate variations with time (lower graph, second order pressure drops are numbered from 1 to 8 and figured in red on the pressure curve).

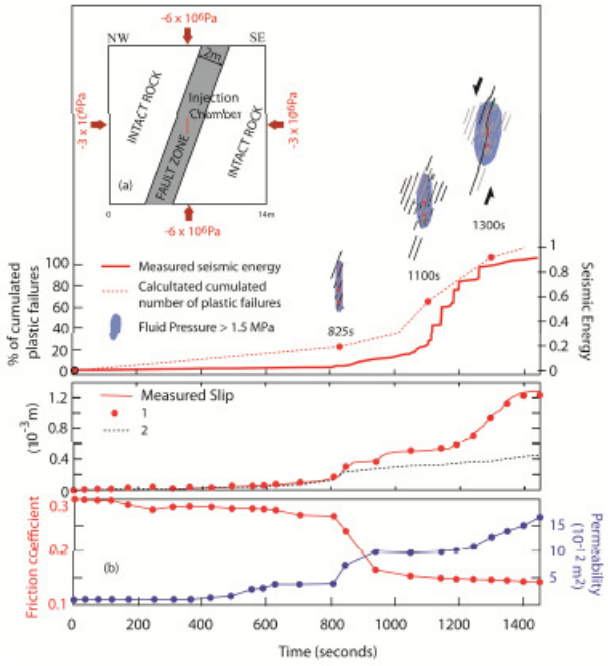

Figure 10: The 2D plane strain numerical fault zone model and fault permeability and friction variations. In the middle graph, red points illustrate the numerical estimations of fault slip when frictional weakening and permeability variations are allowed, and dashed line when frictional weakening but no permeability variations is allowed.

What does this field experiment tell about what will happen in a re-activated fault:

- The evolution of the ratio between the size of the zones where slow slip is controlled by material weakening and the size of the zones that are invaded by high pressure fluids is a key parameter to characterize seismic nucleation in fault zones.

- Slip periods may be either seismic or aseismic but they systematically generate pressure drops which characteristics could be used to estimate the scale of the activated heterogeneities in a fault zone and whether or not they contribute to a macro-rupture nucleation.

- Tremor events are related to the propagation of slow slip on large fault segments preceding high permeability fluid migration. Tracking these low frequency, low amplitude and long duration events (=**fore shocks**) may be critical to detect pulses of fluid leakage (=**main shocks**) within reservoir/cap rock systems.

5 Conclusions

1. Most man-made water reservoirs in the world do not show any sign of reservoir induced seismicity (RIS). Those that do are most often affected by geological faulting or have been constructed in places where contrasts in mechanical rock properties exist in the subsurface.

2. All case studies indicate that, whether RIS will occur or not depends on a number of complex and interrelating factors, such as reservoir size (dam height and volume), reservoir fill histories, fault regime, rock types, and hydrogeological conditions. A combination of these factors is required to trigger seismicity, of which no single factor has an overwhelming control.

3. The mechanisms that cause RSI in fault zones are pore pressure diffusion and changing mechanical rock properties. Depending on fault intensity and tectonic style, earthquake sequences may deviate from the norm (e.g., longer fore- and aftershocks and more intense main shocks).

4. Pore pressure variation due to reservoir impoundment can induce initial seismicity as well as protracted seismicity, as the average pore pressure within the system may continue to increase during the cycles despite the lowered oscillation pore pressure peaks immediately below the reservoir.

5. The mechanical properties of the rock involved, frequency of oscillation and rate of increase of pore pressure influence the growth of seismicity and control the amount and size of the protracted RIS

6. In highly porous and highly permeable rocks, no protracted seismicity or fault reactivation will occur, as almost instantaneous equilibrium will be established below the water reservoir after impoundment as pore pressures can diffuse easily. In low permeability rocks, pore pressure diffusion will be hindered as indicated by the observed phase shifts in experiments. Under these conditions, fault reactivation will occur and foreshock sequence will develop.

7. Oscillating pore pressure, compared to a step increase in pore pressure, can tighten the rock by inducing progressive shearing, which may slow down the pore pressure development in the system and extend the period of seismicity.

8. If the rate of pore pressure increase during reservoir impoundment can be controlled at a slower rate, then induced seismicity is less likely to occur.

To investigate if these (or similar type of) earthquake triggering mechanisms at faults are applicable to induced seismicity in the Groningen gas field a detailed geo-mechanical model that combines fault-structures, reservoir details, and dynamic well data would need to be developed.

6 References

Summary publications

Qiu, Y X., 2012, Factors controlling the occurrence of reservoir-induced seismicity 1st Civil and Environmental Engineering Student Conference, 25-26 June 2012, Imperial College London,

Ying, W.L., 2010, Laboratory simulation of reservoir-induced seismicity, Thesis, Graduate Department of Civil Engineering University of Toronto, 2010

RIS case histories *(Note: all used but not always referenced in this document)*

Assumpcao, M. et al., 2002, Reservoir induced seismicity in Brazil, Pure applied geophysics, vol. 159, p. 597-617.

Chen, L., and P. Talwani, 2001, Mechanism of Initial Seismicity following Impoundment of the Monticello Reservoir, South Carolina, Bull. Seismol. Soc. Am., vol. 91, p. 1582– 1594.

Dahy, S. A., 2012, A Study on Shallow and Deep Focus Earthquakes and Relationship to the Water Level in the Western Side of the Aswan High Dam Lake, Egypt, Research Journal of Earth Sciences vol. 4 (2): p. 63-68.

Federico, Torcal et al., 2005, Induced seismicity around the Tous New Dam, Spain, Geophysics. J. Int., vol. 160, p. 144–160.

Gibson, G., Earthquakes and dams in Australia
Seismology Research Centre, RMIT, PO Box 71, Bundoora, Vic 3083

Guglielmi, Y. and Henry, P., 2013, Relationships between slow slip, seismicity and fluids leakage during a pressurized fault zone rupture in situ experiment (France): Importance for reservoir/caprock stimulation monitoring and efficiency assessment, American Rock Mechanics Association, ARMA 13-517.

Kumar, J. P. et al., 2012, The relation between seismicity and water level changes in the Koyna–Warna region, India, Nat. Hazards Earth Syst. Sci., 12, 813–817.

Main I. G., et al. 2007, The Statistical Reservoir Model: calibrating faults and fractures, and predicting reservoir response to water flood (Gullfaks, UK), in Jolley, S. J., et al. (eds) Structurally Complex Reservoirs,Geological Society, London, Special Publications, vol. 292, p. 469–482.

Mogi, K., 1963, Some discussions on aftershocks, foreshocks and earthquake swarms ‐ the

fracture of a semi-infinite body caused by an inner stress origin and its relation to the earthquake phenomena (third paper). Bull. Earthquake Res. Inst. Vol. 41, p. 615-658

do Nascimento, A. F., 2005, Lunn, R. J. and Cowie, P. A.. Modelling the heterogeneous hydraulic properties of faults using constraints from reservoir-induced seismcity. J. Geophys. Res. v110.

Nghia Quoc Trinh and Krishna Kanta Panthi, 2014, Evaluation of Seismic Events Occurred after Filling and Drawdown of the Reservoir at Song Tranh 2 HPP, Vietnam

Saar, M. O. and Manga, M., 2003, Seismicity induced by seasonal groundwater recharge at Mt. Hood, Oregon, Earth and Planetary Science Letters vol. 214 p. 605-618.

Selim, M. M. et al., 2002, Statistical investigation of reservoir-induced seismicity in Aswan area, Egypt, Earth Planets Space, vol. 54, p. 349–356.

Talwani, P. 1997. On the nature of reservoir-induced seismicity. Pageoph. Vol.150. p. 473-492.

Telesca, L. et al., 2012, Analysis of the cross-correlation between seismicity and water level in the Aswan area (Egypt) from 1982 to 2010, Nat. Hazards Earth Syst. Sci., vol. 12, p. 2203–2207.

Note on simulation model pressure response for high frequency production swings

October 2015

Peaks in gas production lead to pressure transients in the reservoir. To test the impact of intra-day swings as a pressure response at fault planes, a reservoir simulation was run with hourly timesteps.

The GFR2015 model was used with the extended grid (Figure 1).

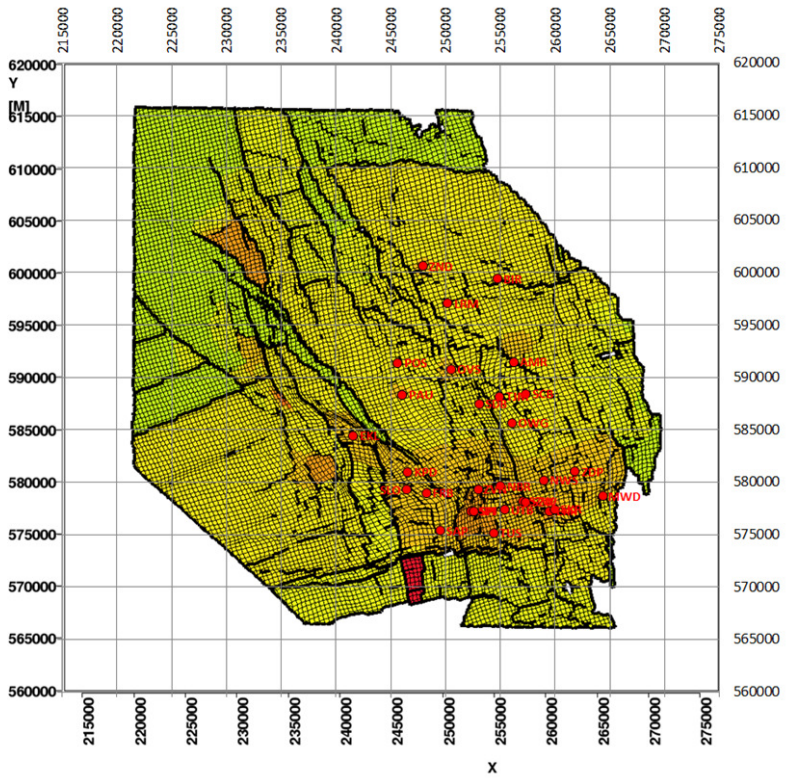

Figure 1: Simulation grid from the GFR2015 model

Observation wells were defined in the model around the De Eeker clusters, with each observation well defined as a vertical well penetrating a column of gridblocks. Consequently, each of these observation wells tracks the pressure for a set of X,Y coordinates. A matrix (row-column) naming convention was used, e.g. 11 to 55, with a total of 25 observation points (Figure 2).

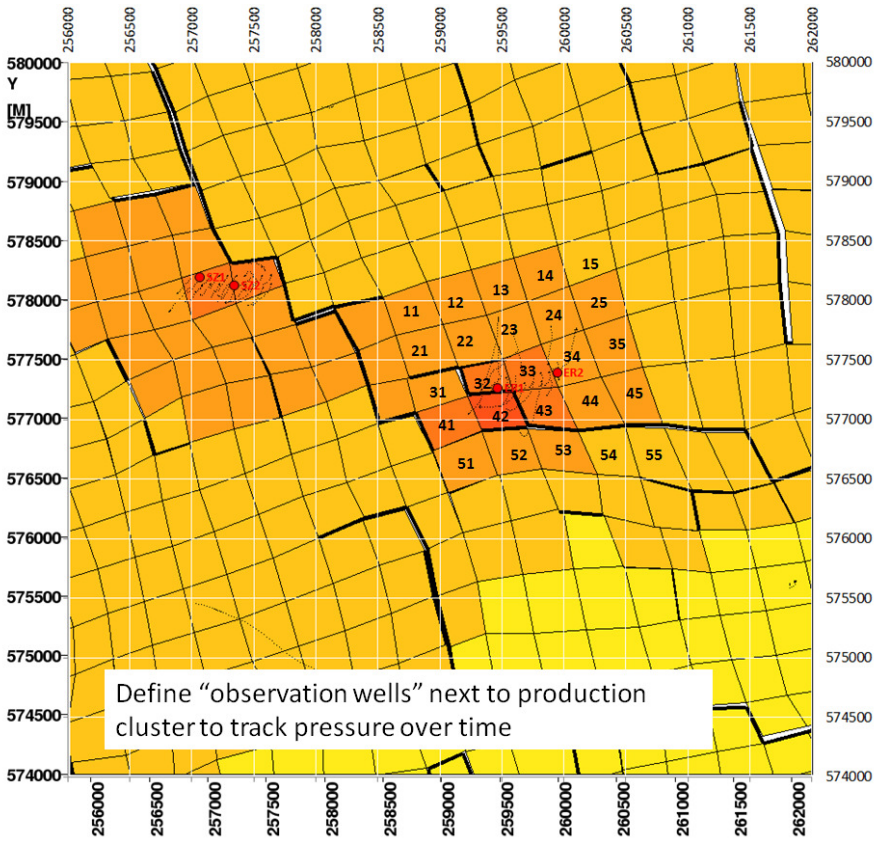

Figure 2: Zoom of GFR2015 simulation grid around De Eeker clusters, with observation wells indicated (naming convention in matrix format)

Normal simulation runs are done in monthly timesteps. When refining to hourly timesteps there is an increase of some 720 fold in the number of timesteps (30d x 24h/d). Therefore, a relatively short period was selected for this analysis: the production period Feb-Mar 2013 (Appendix 1). A consequence is that the volume withdrawal over a timestep also reduces by a factor of some 720.

The simulated production history is given in Figure 3. The intra-day swing can be clearly observed from the production data; gridlines are set at roughly 1 week (0.02 year ~ 1 week).

> Note that a QC step of the production data is given in Appendix 2. The unreconciled hourly data was compared to the reconciled corporate database, and was found to be highly congruous.

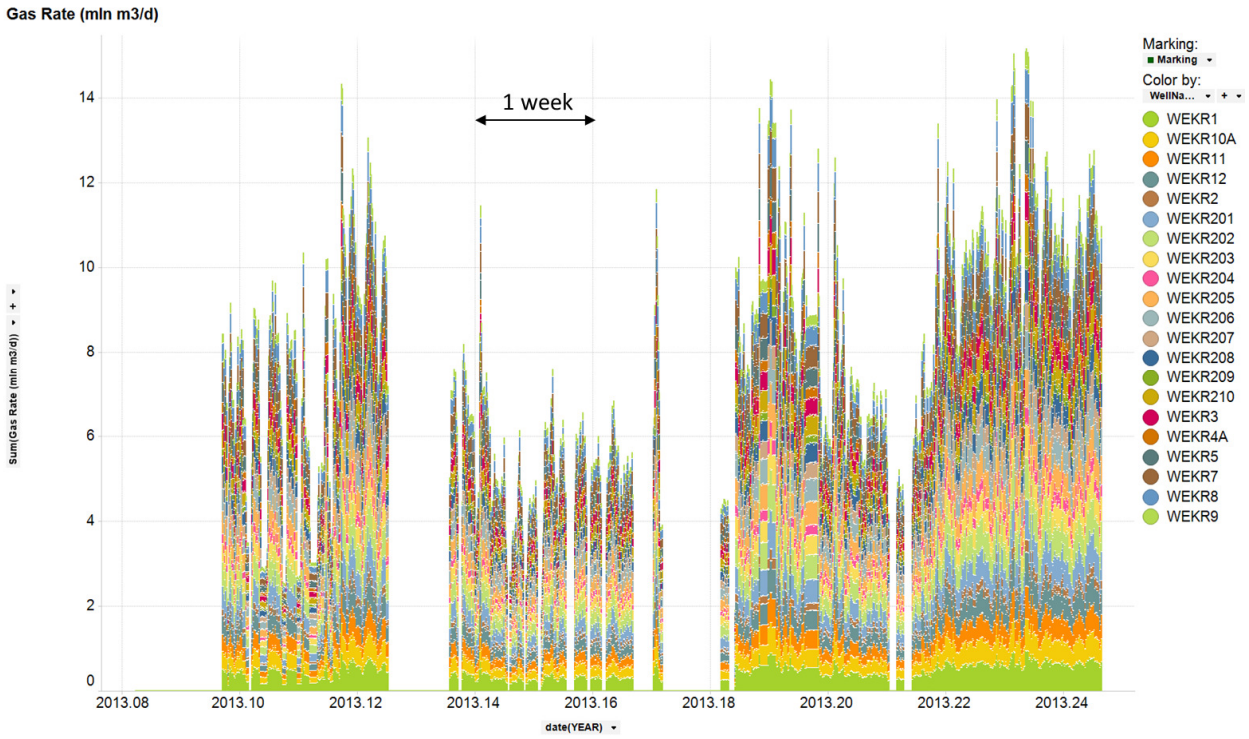

Figure 3: Hourly production data by well for De Eeker clusters over the period February-March 2013

The simulated pressure response to the hourly offtake is given in Figure 4[1]. It can be observed that the drawdown of the producing wells is fairly limited (up to some 5 bars). In the gridblocks that are directly penetrated by production wells, the pressure response due to the daily fluctuations is limited to some 0.2 bars. It is more pronounced as a result of the shutdowns, which show pressure build-ups of up to 4 bar within a week.

One gridblock away from the producing wells, the pressure is already becoming a lot smoothened, and the intra-day fluctuations are dampened out.

Two gridblocks away from the producing wells, the pressures are smoothened even further (and can even become monotonously decreasing)

A reporting script was included in the simulation which calculates the average reservoir pressure at datum level per production cluster. The script establishes a range of gridblocks around the production cluster that represents a drainage radius of 3 days (roughly some 1km). Figure 5 gives the associated gridblock ranges for respectively De Eeker-1 and De Eeker-2 cluster, and the averaged pressure response over those ranges. Again, the intra-day pressure response is roughly averaged out.

[1] Note that the pressures for both the production and observation wells are reported at pump height, which is set at the top of perforations (different for each well).

Figure 4: Pressure response for selection of wells and gridblocks

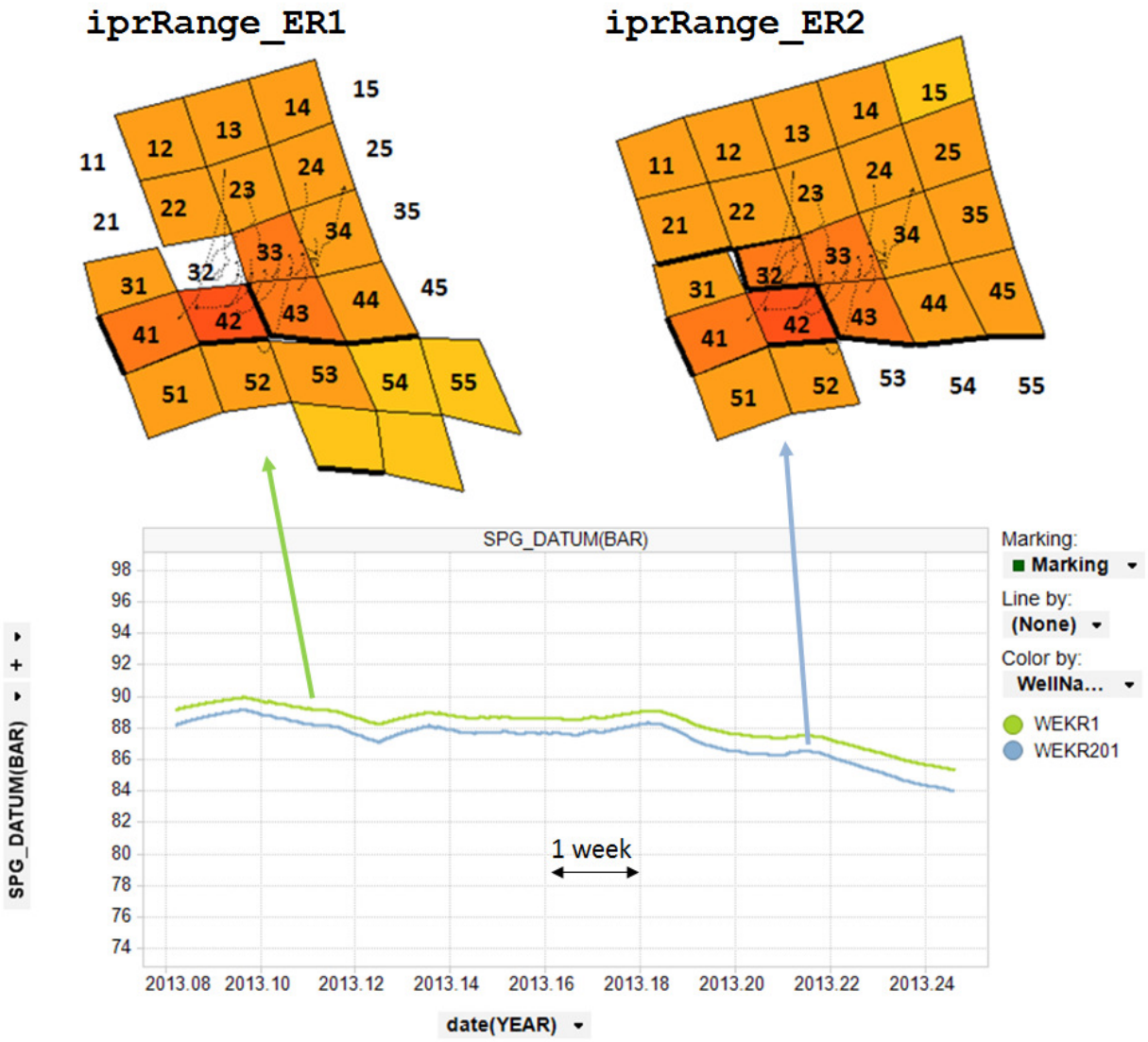

Figure 5: Pressure response averaged over a 3-day drainage radius, at datum (2875mTVDSS)

In conclusion, only wells that are in close proximity to a fault plain (<500m) will exert a measurable pressure on the fault plain (>0.2 bar). Further away from the wellbore the pressure response gets significantly dampened.

For more granularity it is recommended to do a similar analysis analytically using welltest software.

Appendix 1 – Selected production period

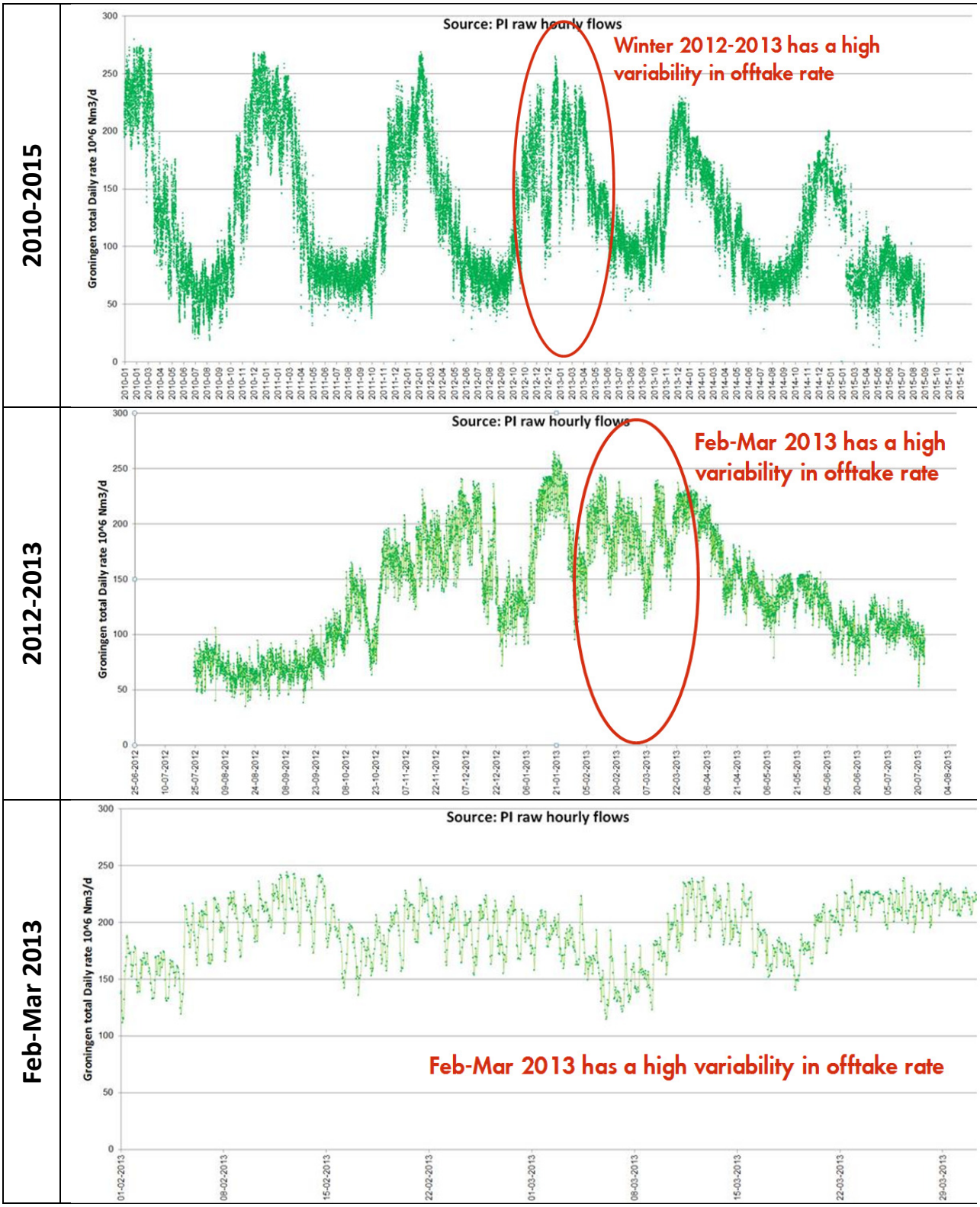

AANTAL AARDBEVINGEN IN HET GRONINGEN-GASVELD

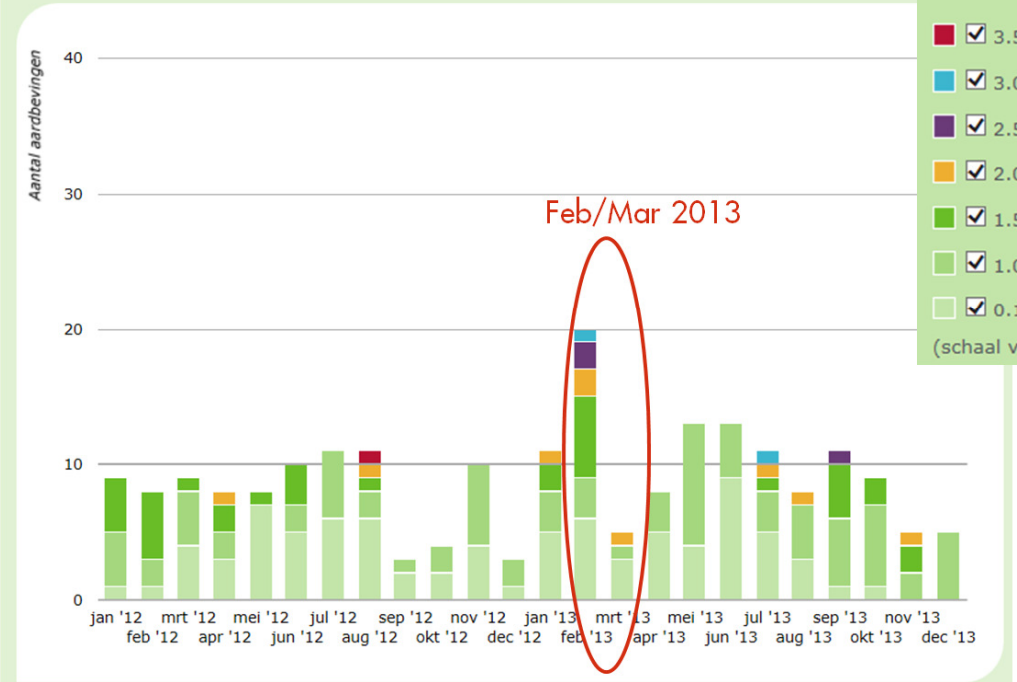

SELECTEER STERKTE AARDBEVINGEN

- ☑ 3.5 en hoger
- ☑ 3.0 tot 3.5
- ☑ 2.5 tot 3.0
- ☑ 2.0 tot 2.5
- ☑ 1.5 tot 2.0
- ☑ 1.0 tot 1.5
- ☑ 0.1 tot 1.0

(schaal van Richter)

Appendix 2 – QC of production data

The hourly daily data from the online flowmeters is un-reconciled. When comparing the averaged rates to the official allocated production as reported in Energy Components, the rates match very closely (within 0.2% for Feb/Mar), see Figure 6.

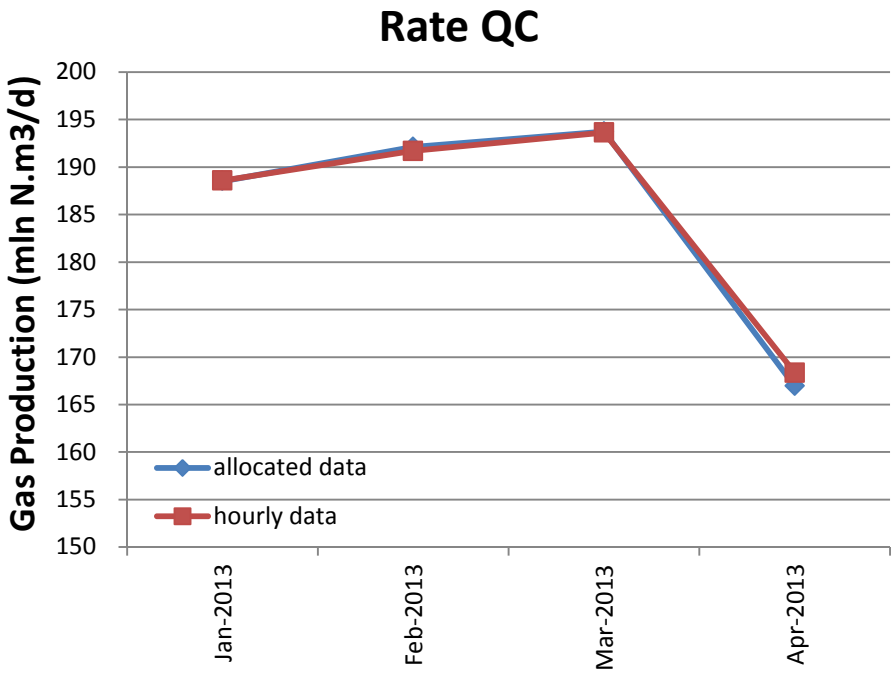

Figure 6: QC of production data

ExxonMobil

Pressure Disturbance Estimation for Variable Production at Groningen

Illustrative Calculations

Energy lives here™

October 29, 2015

Bill Symington, ExxonMobil Upstream Research Company

DRAFT

Pressure Disturbance Estimation for Variable Production at Groningen

ExxonMobil Upstream Research

These calculations are intended to help frame discussion of the likelihood that variable production rates from Groningen wells can impact on earthquake frequency. The calculations assume a single well in an infinite-acting, compressible gas reservoir. While the calculations are approximate, they should reflect the pressure drawdown near wells to first order. Key points concerning the calculations include the following:

- Rock and flow properties have been taken from estimates for the field as a whole. Several of the values used come from the Technical Addendum to the 2013 Winningsplan.
- The base case properties include a permeability of 150 mD. Lower-perm and higher-perm cases were also run at 50 mD, and 450 mD (3X-higher and 3X-lower).
- The steady production rate was estimated assuming a field wide rate of 35 billion Nm3 per year and 297 wells. The steady rate calculates to roughly 32000 reservoir bbls/day.
- For the base case, at locations very near the well (say 25 feet away) the drawdown is minimal, about 4 psi after 2 years.
- To simulate variable rate production, the average rate was doubled and switched on and off every 12 hours. Drawdowns close to the well (25 feet) increased to about 5 psi after 10 days. As close as 400 feet from the well it becomes difficult to see the 12-hour variation in the drawdown. At 1000 feet the daily pressure wiggle is minimal.
- Even for the lower permeability case, drawdowns are still quite modest: about 12 psi after 2 years at 25 feet (steady flow), or about 15 psi at 25 feet after 10 days of variable production.
- All these drawdowns are very small compared to the general reservoir depletion of about 250 bars (3626 psi) that has already occurred in the field.

DRAFT

Pressure Disturbance Estimation for Variable Production at Groningen

ExxonMobil Upstream Research

Fluid Flow Properties of a "Typical" Groningen Producer

Property	Symbol	Value
Permeability	k	150 md
Porosity	ϕ	0.12(1)
Gas Viscosity	μ_g	0.0157 cp
Young's Modulus	E	15 Gpa
Poisson Ratio	v	0.18
Rock Compressibility	C_R	3.62×10^{-6} 1/psi
Gas Compressibility	C_g	7.65×10^{-4} 1/psi
Total Compressibility	C_T	7.69×10^{-4} 1/psi
Diffusivity	η	655,520 ft^2/day
Gas density (standard conditions)	$\rho_{g\ (std)}$	0.000787 g/cc
Gas density (reservoir conditions)	$\rho_{g\ (res)}$	0.0598 g/cc
Production Rate	Q	32000 res-bbls/day
Reservoir Thickness	h	250 meters
Δp scaling	$Q\mu_g/4\pi kh$	0.288 psi
Initial pressure	p_{init}	1377.86 psi
Reservoir temperature	T_r	100 °C

(1) Reflects gas-filled porosity

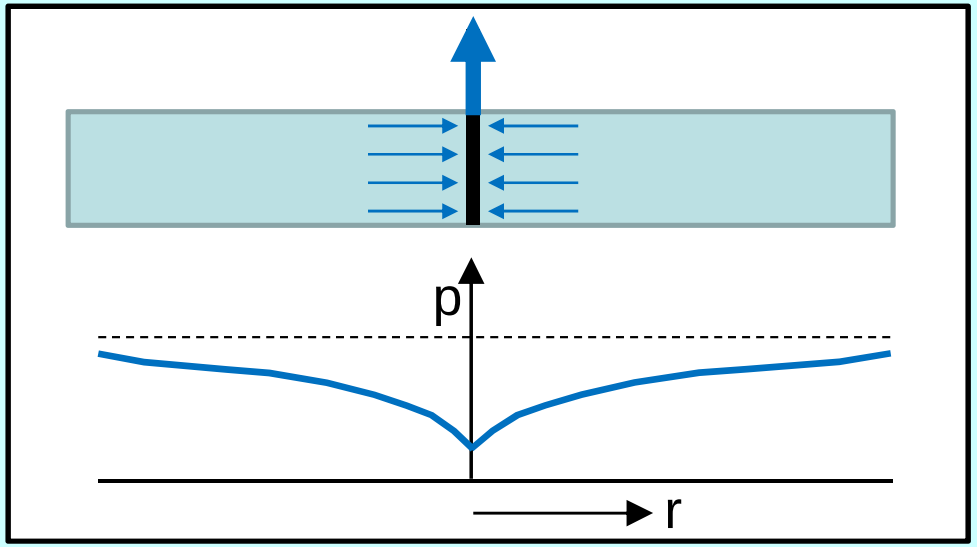

Wellbore pressure given by:

$$p = p_{init} - \frac{Q\mu}{4\pi kh}\left\{E_1\left(\frac{r_w{}^2}{4\eta t}\right)\right\}$$

Average well production:

322.9 kNm^3/day	(35 GNm^3/yr, field-wide(2))
11.4 Mscfd	(convert to scf)
150.3 k-res-ft^3/day	(convert to res-ft^3)
26.77 k-res-bbls/day	(convert to res-bbls)
32.0 k-res-bbls/day	(correct for 14% N_2 in gas)

(2) assumes 297 wells

DRAFT

Pressures Surrounding a Groningen Producer

ExxonMobil Upstream Research

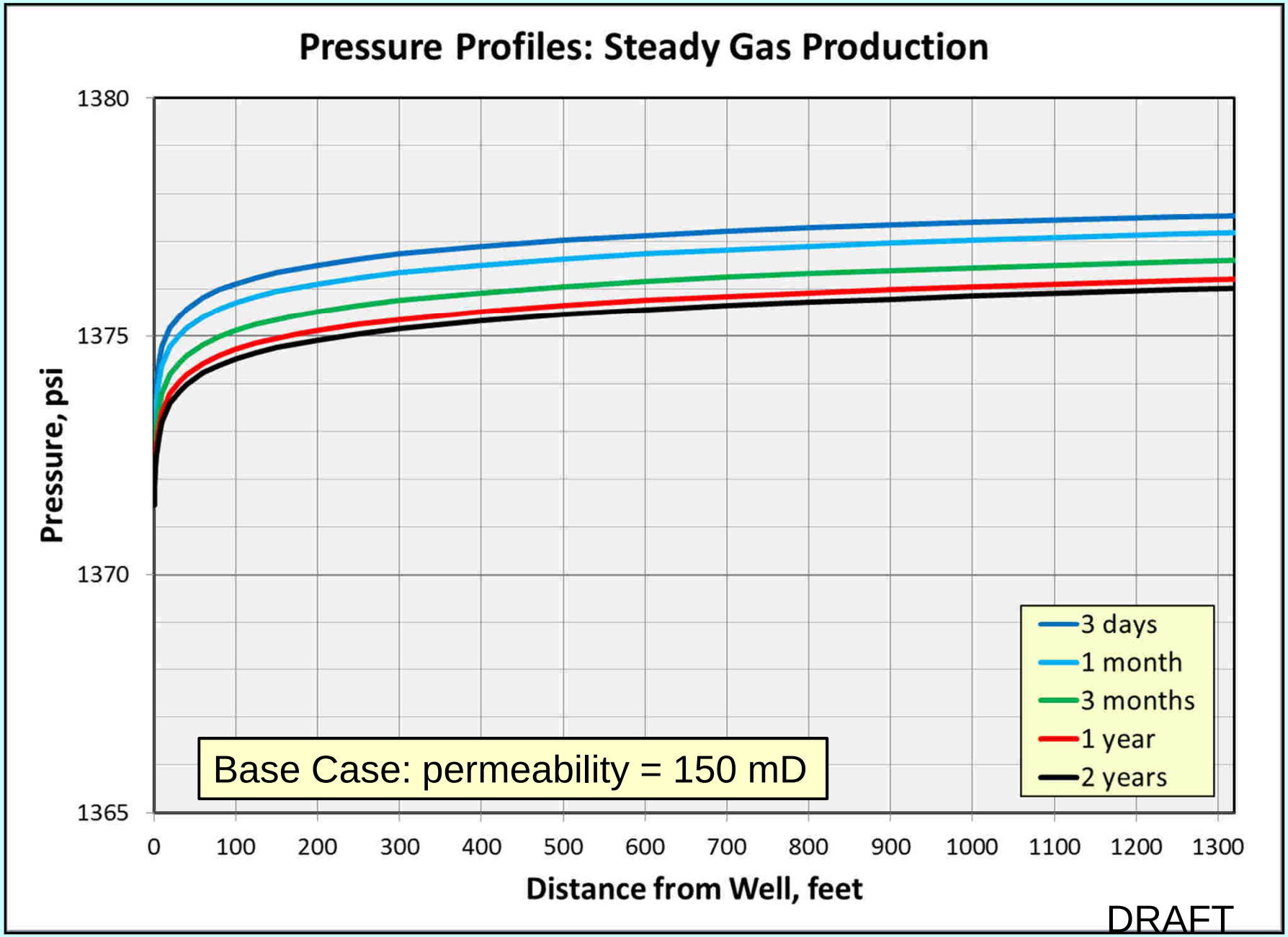

Pressures Surrounding a Groningen Producer

ExxonMobil Upstream Research

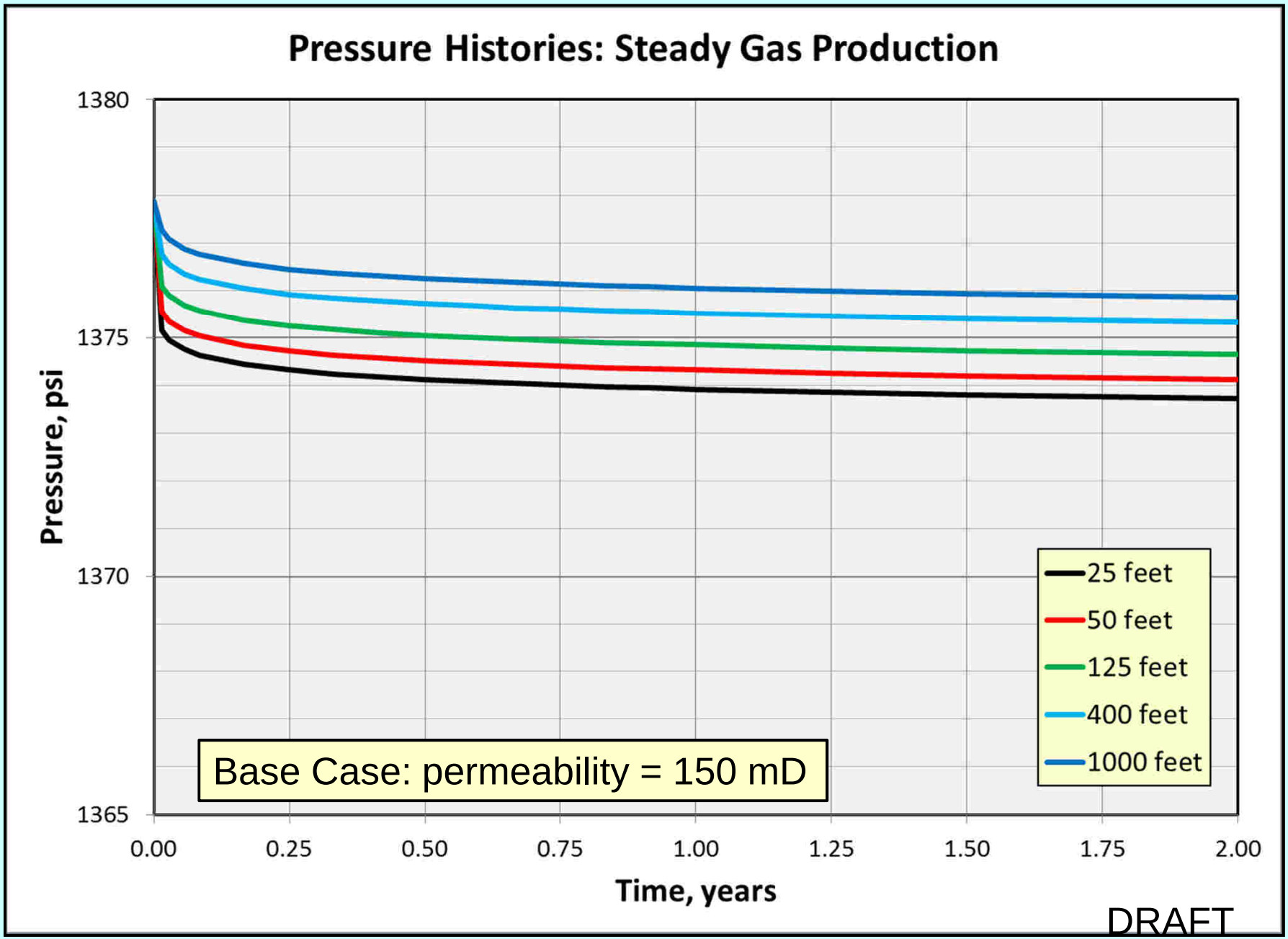

Pressures Surrounding a Groningen Producer

ExxonMobil Upstream Research

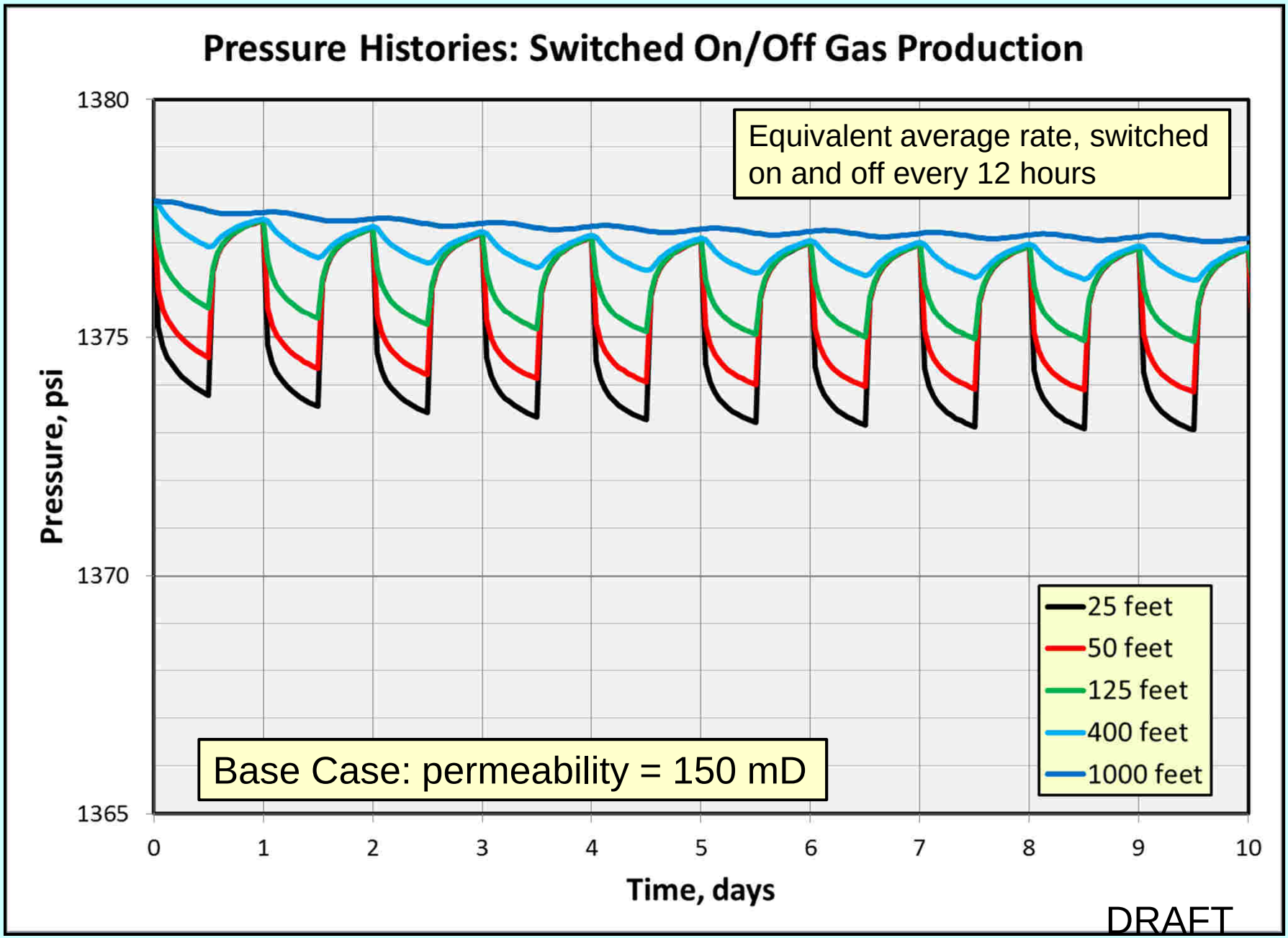

Pressures Surrounding a Groningen Producer

ExxonMobil Upstream Research

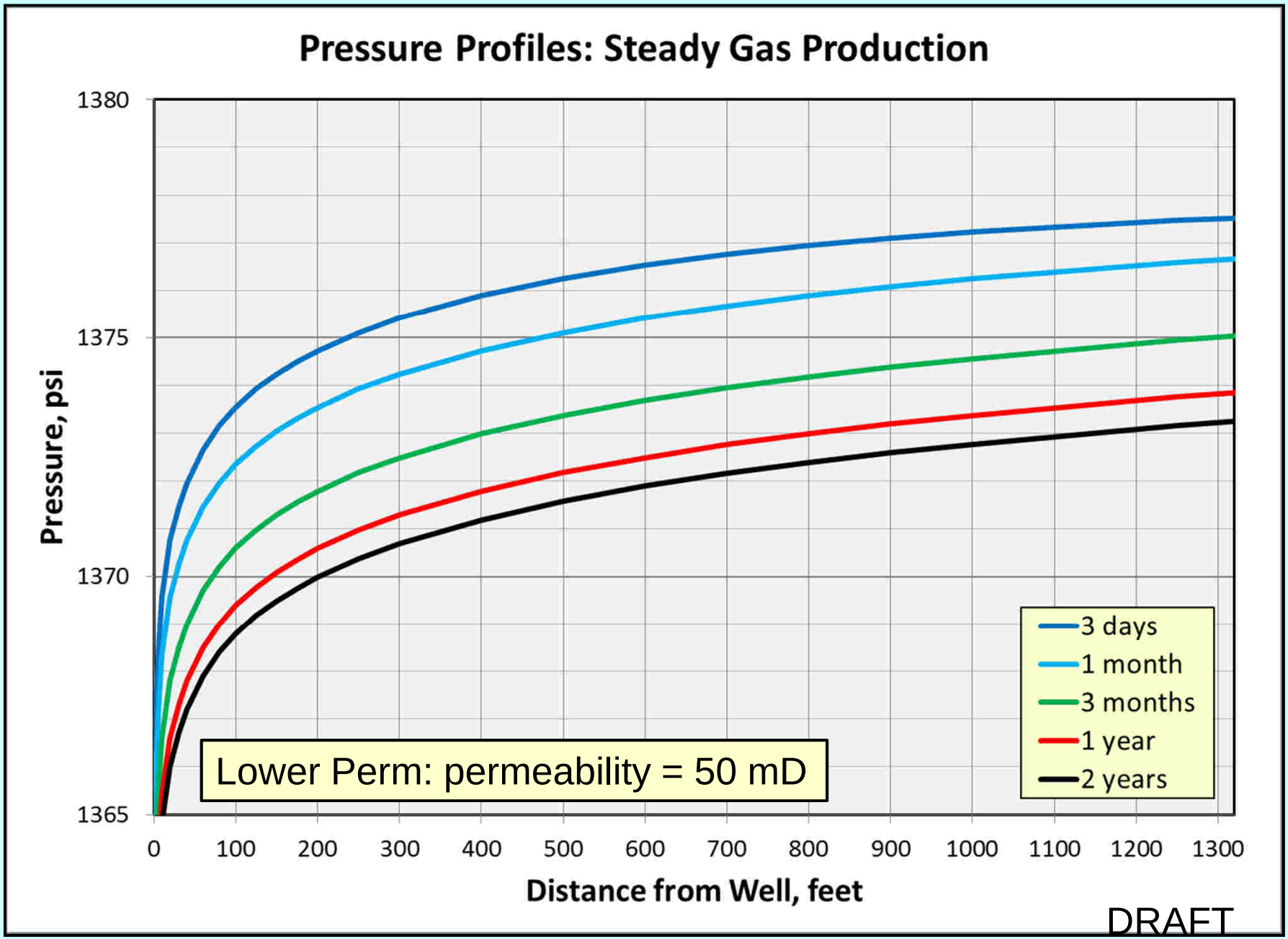

Pressures Surrounding a Groningen Producer

ExxonMobil Upstream Research

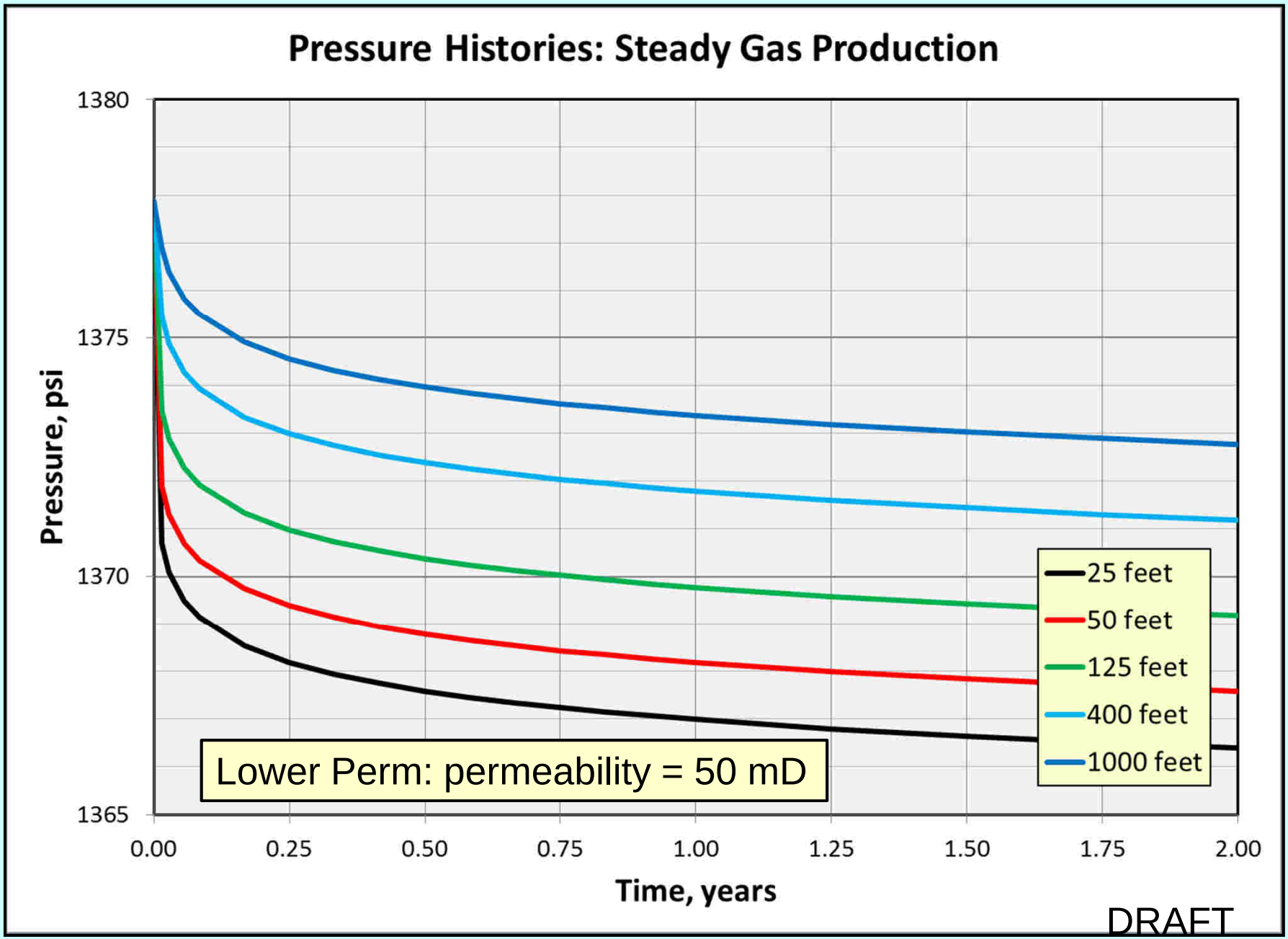

Pressures Surrounding a Groningen Producer

ExxonMobil Upstream Research

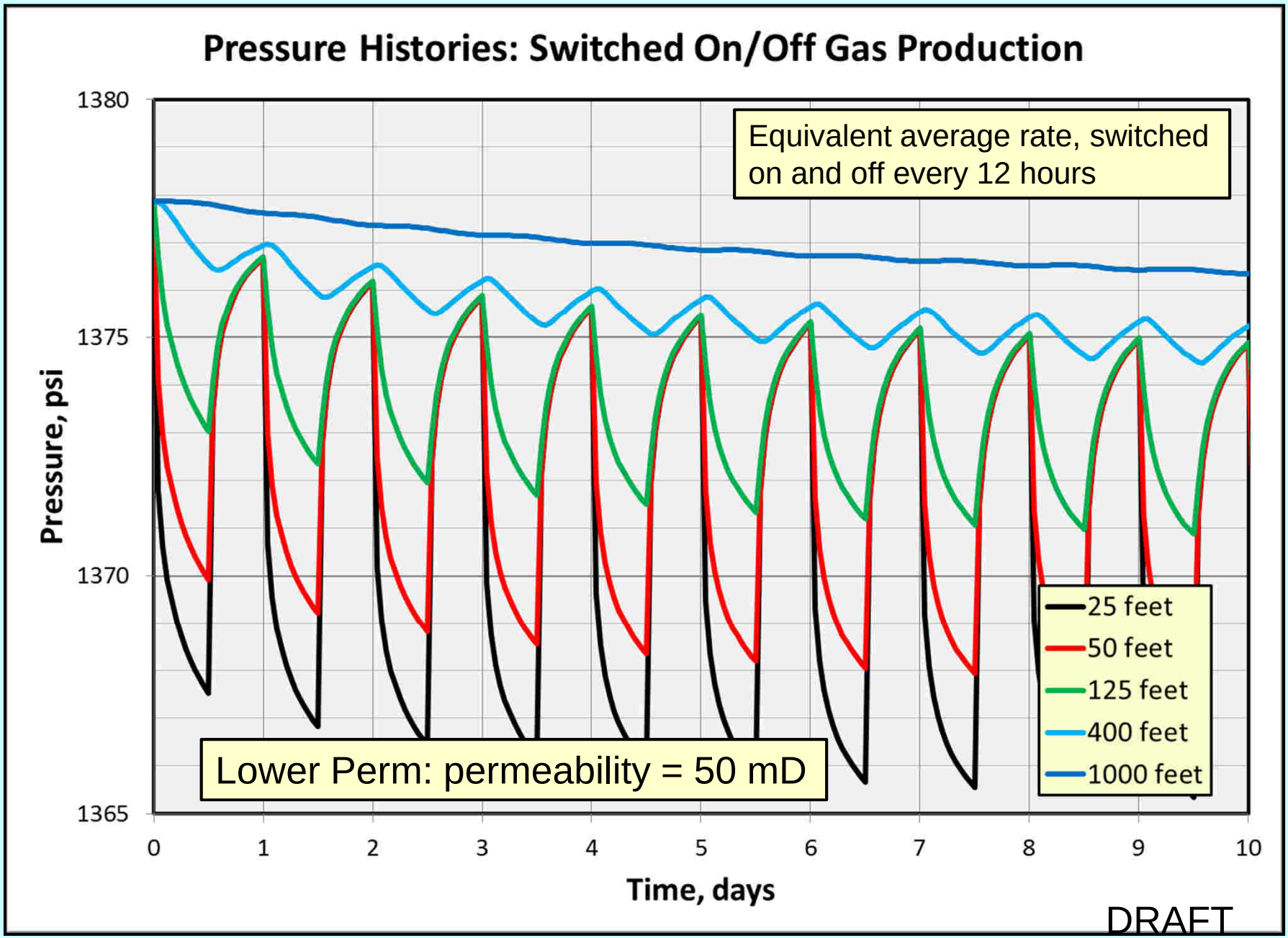

Pressures Surrounding a Groningen Producer

ExxonMobil Upstream Research

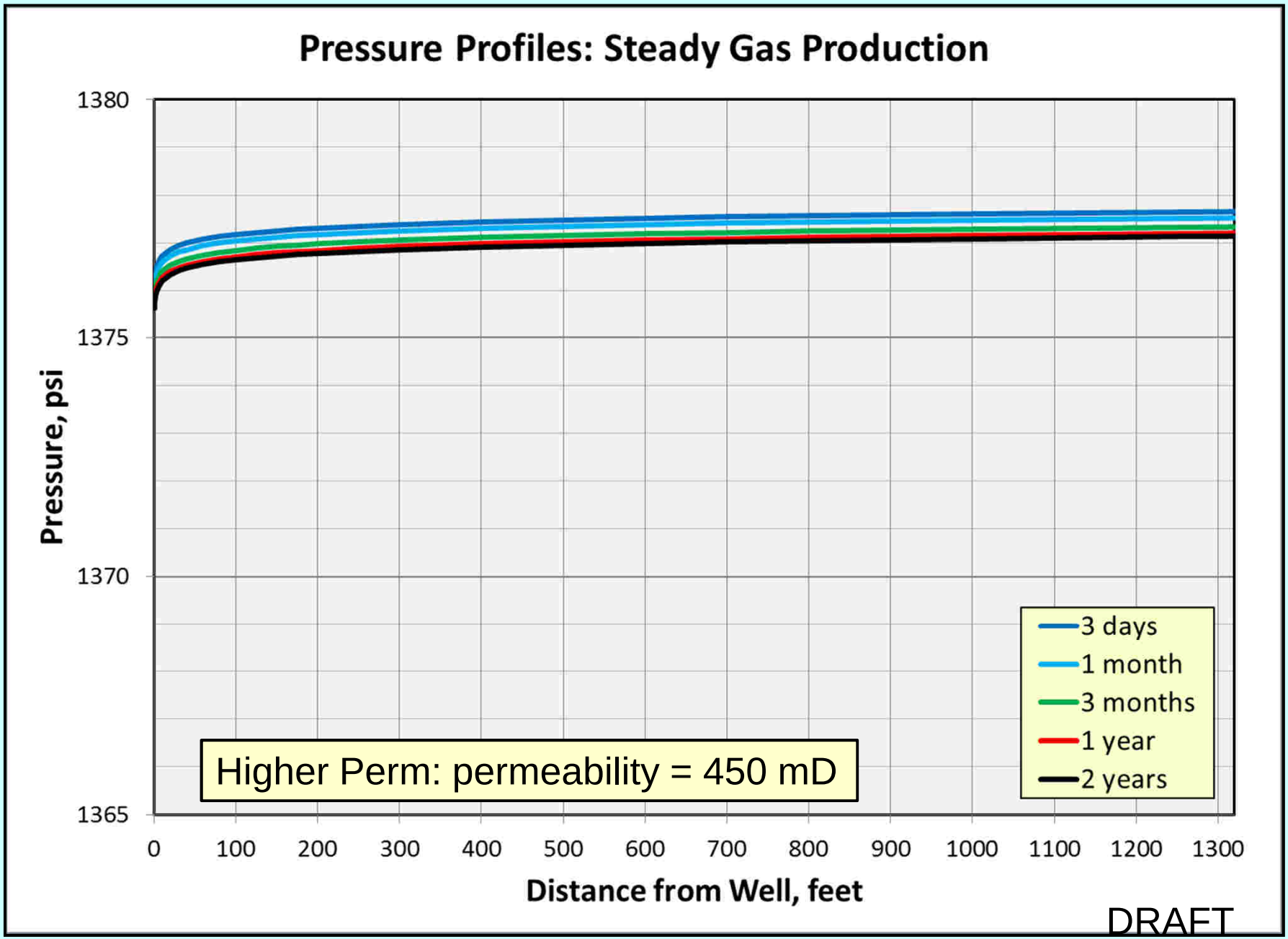

Pressures Surrounding a Groningen Producer

ExxonMobil Upstream Research

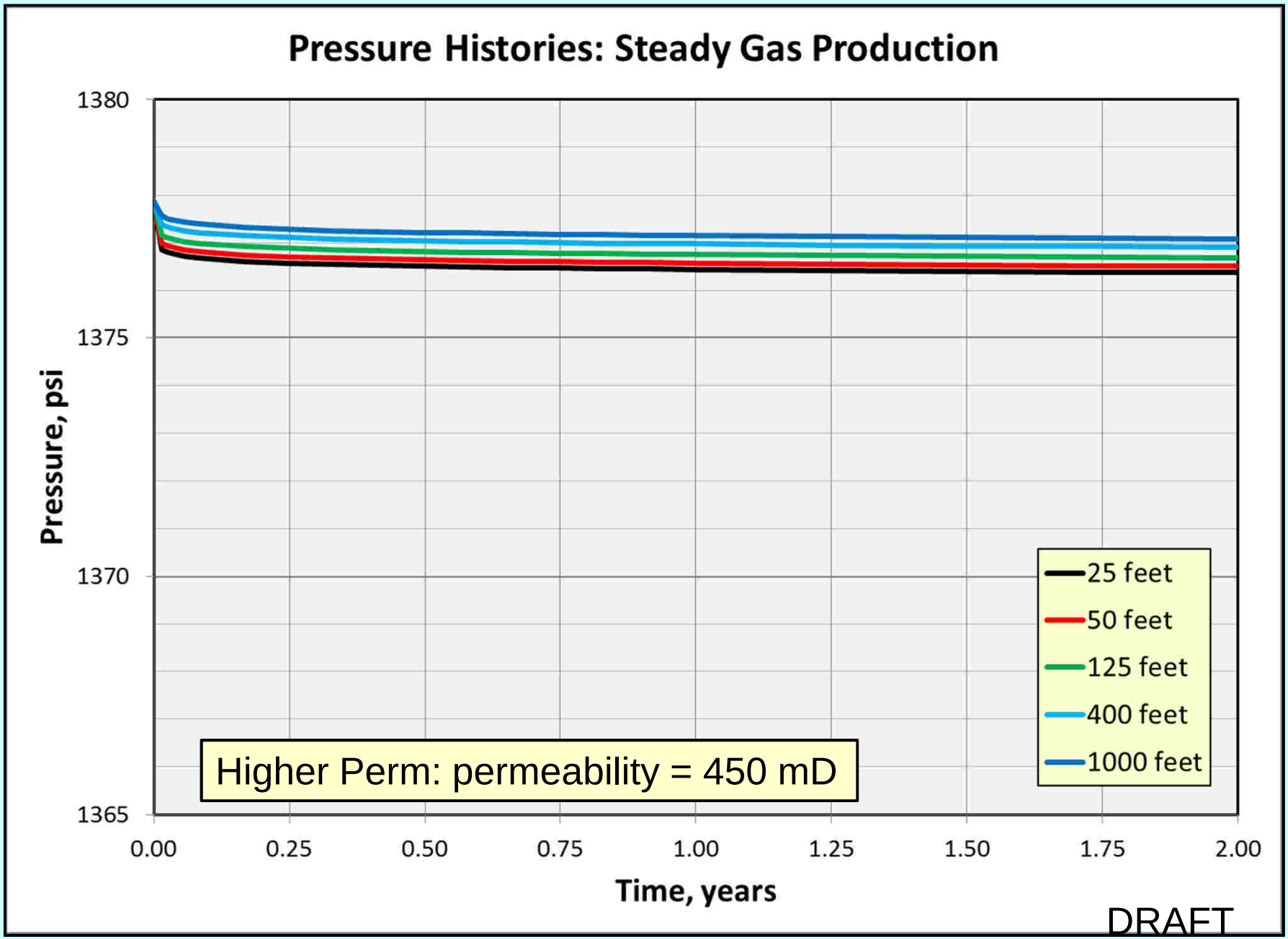

Pressures Surrounding a Groningen Producer

ExxonMobil Upstream Research

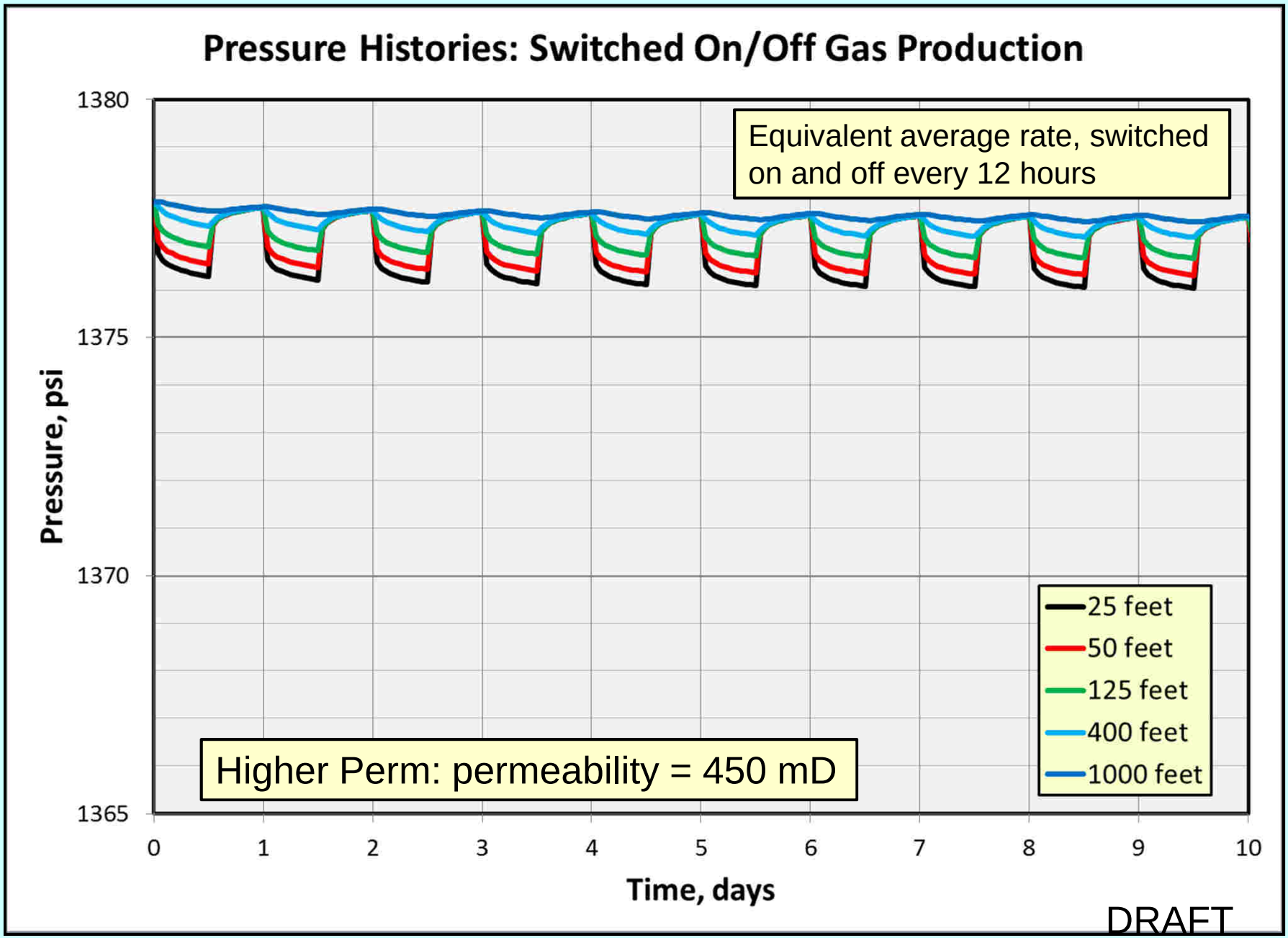

Historical Groningen Gas Production

ExxonMobil Upstream Research

DRAFT

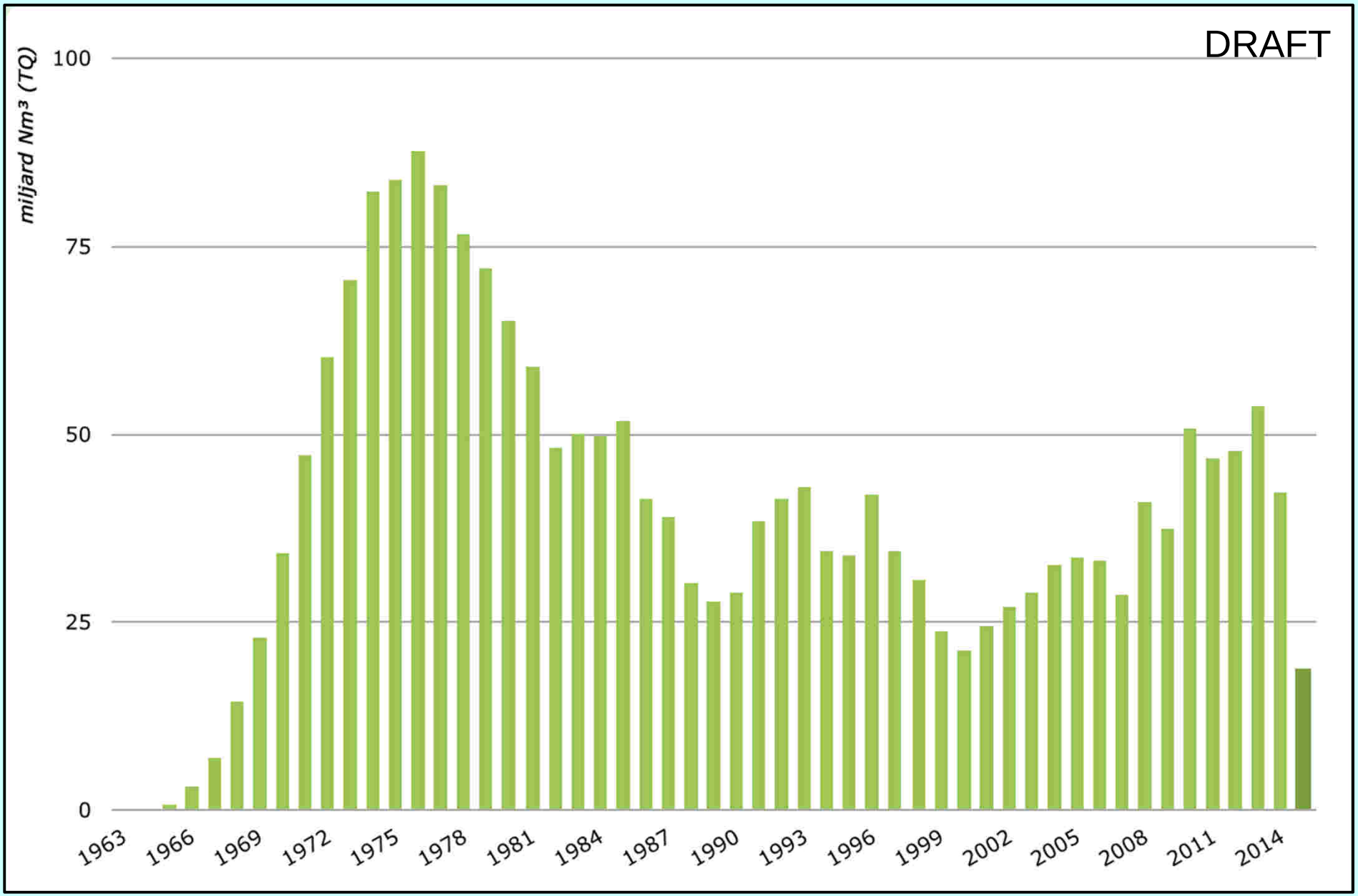

Source: http://feitenencijfers.namplatform.nl/gaswinning/

Faults and Earthquakes

Shell Global Solutions, November 2015

This note describes a fault rupture mechanism based on geomechanical principles that can explain the occurrence of earthquakes in depleting reservoirs.

Groningen faults

From a geomechanical point of view, faults are considered planes of weakness relative to neighbouring formations. The geological model of the Groningen field includes 1037 mapped faults (Visser, 2012), which intersect with the depleting Slochteren reservoir formation (Figure 1). The Slochteren reservoir is offset along these faults between 0 and 150m at most locations, which is about half the reservoir thickness. Many more faults are present within, and intersecting with the Slochteren reservoir, but have not been interpreted because their size or offset is too small to be detected on 3D seismic. The relative weakness of faults and the proof that some earthquakes in the Groningen field have occurred along known fault planes causes the geomechanical assessment to focus on the behaviour of faults under depleting reservoir conditions.

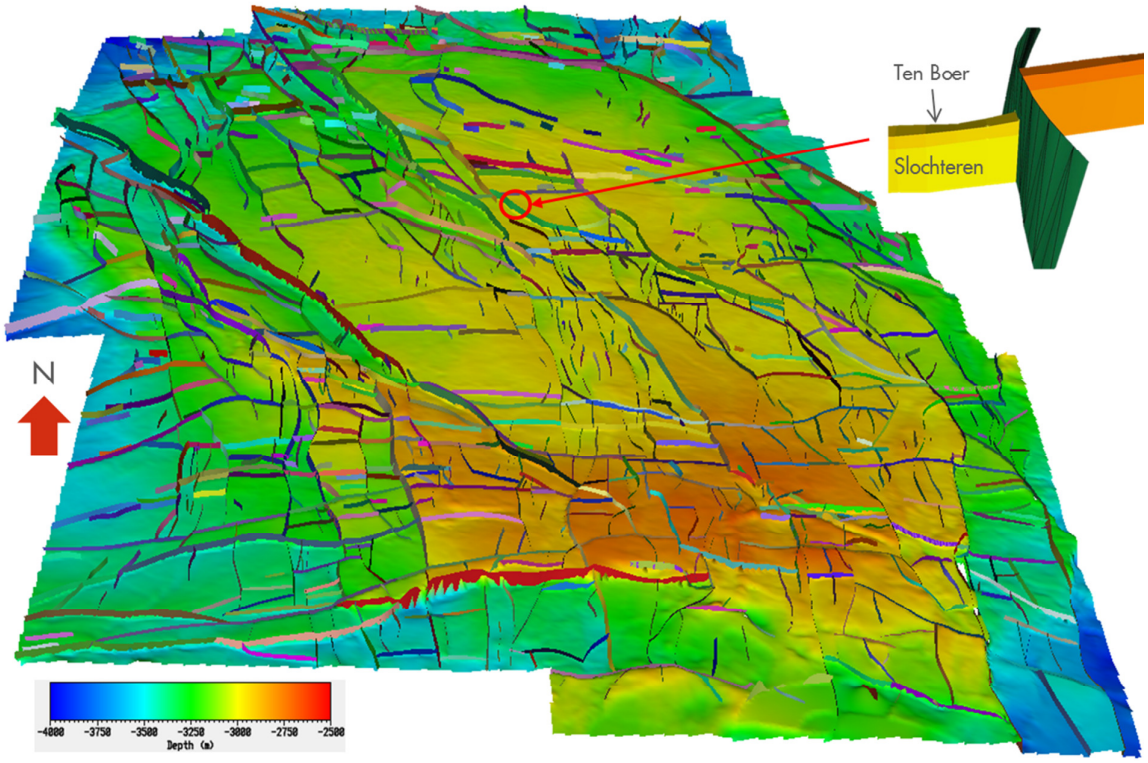

Figure 1 *The 1037 mapped faults in the Groningen field projected on the top Carboniferous depth map. The detail shows an example of vertical offset of the Slochteren formation across the fault.*

Geomechanical modelling

In all engineering disciplines, failure of materials and structures is described by a stress-based criterion. That is, failure is predicted if the loading (stress) exceeds the strength. An earthquake is the evidence that failure has occurred in the subsurface. Faults, which are assumed to have lower strength than its environment, are the natural locations to expect these failure events. The difficulty in predicting natural or induced earthquakes along fault planes is the fact that both loading stress

and strength are (highly) variable and that available data is often inaccurate or too scattered aerially. This is the reason why alternative approaches are followed, such as the one used for Groningen which is based on reservoir compaction and subsidence. Stress-based models are pursued to improve our understanding of the mechanism that causes earthquakes in the Groningen field and to provide a geomechanical basis for an improved seismological model and hazard & risk assessment.

Knowledge of the local stress condition at the fault plane is essential for a stress-based model. Thereto, an estimate of the global stress is required as well as any local disturbance or variation. The global stress response is typically obtained from the world-stress map (see references) and in-field stress measurements, such as leak-off tests (Zheng et al., 2014, for Groningen data). However, local disturbances are often providing a very strong stress over-print and thereby dominate the failure behaviour. For instance, the presence of the borehole perturbs the local stress condition that may lead to bore-hole instability when using an inappropriate mudweight. Also, rapid changes in operating conditions affect the local stress condition, such as rapid well bean-up that may lead to (transient) sand production. Both, borehole instability and sand production issues are explained by local and steep stress gradients. Hence, the mantra of (geo)mechanics could read “steep gradients lead to failure”. This is valid in aerial as well as in temporal sense. For an assessment of fault stability in the Groningen field it may be relevant to incorporate gradients introduced by production fluctuations across the field and over time and caused by offset of depleting reservoir formations along faults.

The importance of reservoir formation offset has been detected in previous work by Roest et al. (1994), Glab et al. (2001), Mulder (2003) and Orlic et al. (2012). Therefore, after the Huizinge earthquake in 2012, a 2-dimensional Finite-Element analysis framework has been developed to evaluate fault stability in the Groningen field for a wide range of modelling options and parameter settings (Figure 2, Van den Bogert, 2015) with the objective to evaluate the fault slip process in detail. Recently, this framework has been extended to also simulate the dynamic rupture behaviour of faults. This analysis capability, which has been benchmarked against other codes, has resulted in new insights into the fault rupture process (Buijze et. al., 2015) that is assumed to cause the earthquakes in the Groningen field.

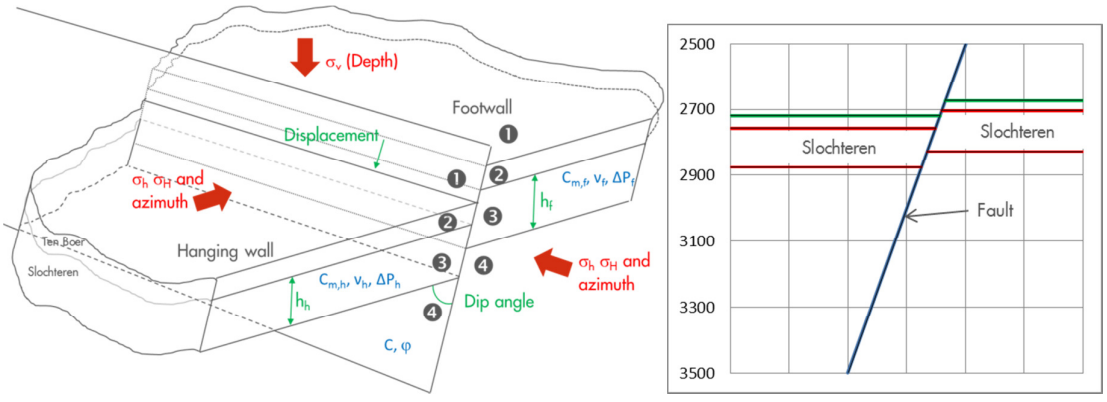

Figure 2 Two-dimensional representation of the depleting Slochteren reservoir that is intersected and offset by a fault.

The following four stages of fault stability can be identified:

Stage 1: No fault slip under increasing reservoir depletion

Stage 2: Stable (a-seismic) fault slip propagation under increasing reservoir depletion
Stage 3: Instable, seismic fault slip (without further reservoir depletion)
Stage 4: Stable (a-seismic) fault slip propagation under increasing reservoir depletion

The first three stages are discussed in the next sections.

Stage 1: increasing reservoir depletion leading to onset of fault slip

Failure occurs at the transition point from Stage 1 to Stage 2, where the stress-based failure criterion is satisfied at some location on the fault plane (figure 3). This point is also referred to as the onset of fault slip. Conventionally, a Mohr-Coulomb shear failure criterion is assumed to specify the maximum shear stress τ_{max} that can be carried by any point along the fault plane. A 2D FE analysis allows assessment of the local stress condition and finding the location at which onset of fault slip occurs, i.e. where SCU = τ / τ_{max} = 1. The graph on the left in Figure 3 shows a relatively uniform distribution of the SCU over the height of the depleting reservoir for the case without offset. This implies that shear stress loading caused by depletion is rather uniformly distributed over the fault and onset of fault slip is found at a more elevated depletion level than for the case with offset that is shown at the right-hand side of Figure 3. The reservoir offset causes a much more concentrated shear stress loading on a small portion of the fault, thereby introducing steep gradients in the shear stress and SCU. Consequently, onset of fault slip is found at a lower depletion level as for the case without offset .

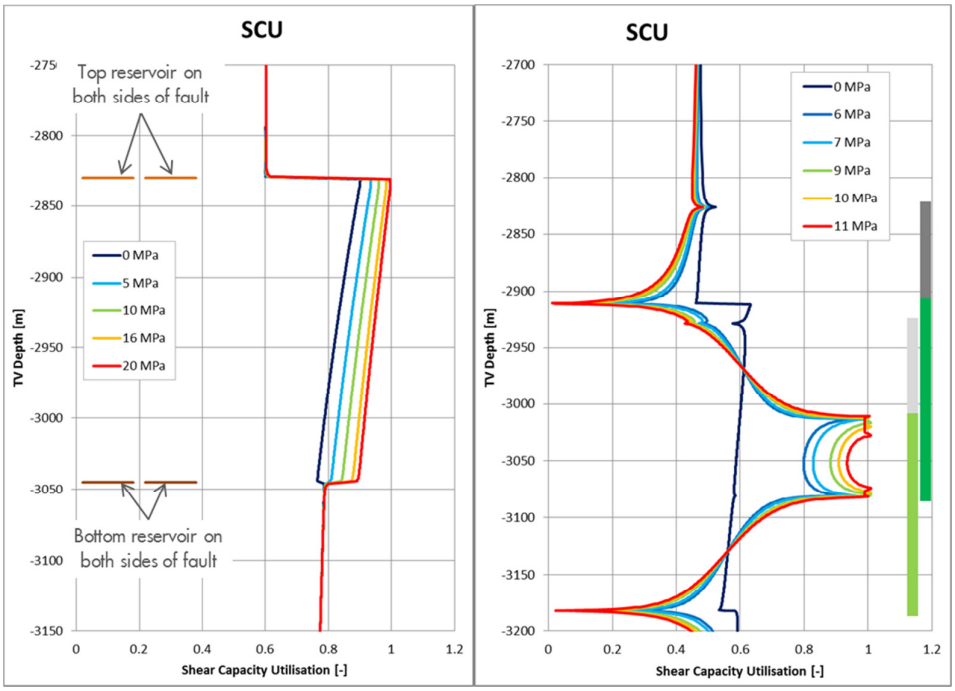

Figure 3 *The Shear Capacity Utilisation is the ratio between the actual shear stress τ and the shear strength τ_{max} and is 1 at the onset of fault slip. Left: the SCU distribution as a function of depth for the case without reservoir offset, with onset of fault slip at 20 MPa reservoir depletion. Right: the SCU distribution for the case with an offset of about half the reservoir thickness, with the onset of fault slip after about 6 MPa reservoir depletion.*

Stage 2: Stable (a-seismic) fault slip propagation under increasing reservoir depletion

The behaviour of the fault after the onset of slip (Figure 4) determines if stable fault slip propagation in Stage 2 may turn into an earthquake (Stage 3) or not. The left-hand side of Figure 4 shows a fault without slip-weakening behaviour, while the right-hand graph shows a linear reduction of the shear

strength τ_{max} from $\tau_{max\text{-}initial}$ at the onset of fault slip to $\tau_{max\text{-}residual}$ once the critical slip displacement D_c is exceeded. A fault remains stable (Stage 2) in the absence of slip-weakening behaviour, and additional reservoir depletion is required to increase the length of the slip patch (Van den Bogert, 2015). Slip-weakening behaviour is required to explain the occurrence of earthquakes (Buijze et al., 2015).

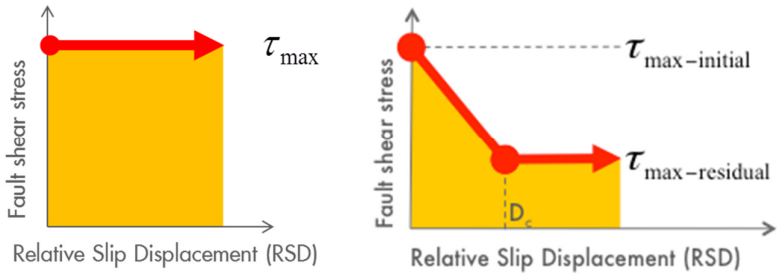

Figure 4 *Two simplified relationships between the fault shear stress and slip displacement. Left: a fault without slip-weakening behaviour. Right: a fault with linear slip-weakening behaviour.*

Let's consider the length of the slip patch for different values for the critical slip displacement D_c (Figure 5). The right-hand side shows that fault slip starts at the top of the depleting reservoir and expands downward upon further depletion. For the green case (D_c=0.05 m), the length of the slip patch expands downward almost 200 m in a stable fashion until 17 MPa depletion. This is indicated by the solid green arrow representing Stage 2. An incremental depletion above 17 MPa will cause the length of the slip patch to jump to about 250 m, which is the entire length of the dipping fault over depleting reservoir interval. This is indicated by the dashed green arrow representing Stage 3. So, a slip patch of almost 200 m becomes unstable and an earthquake is triggered after 17 MPa of depletion if D_c=0.05 m. The same failure mechanism applies for the yellow and red case in Figure 5, except that instable equilibrium occurs at a lower reservoir depletion level and a smaller length of the slip patch. For the considered fault configuration, no instable, seismic fault slip process takes place if D_c > 0.10 m. So, the fault strength should reduce sufficiently quick with increasing slip displacement in order to cause an earthquake (Stage 3).

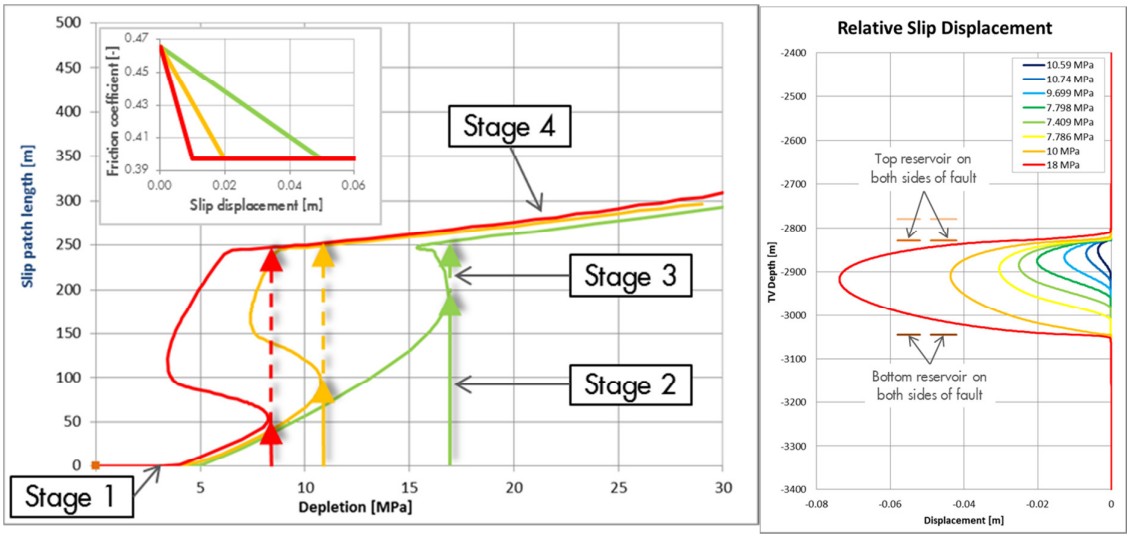

Figure 5 *Left: the length of the slip patch as a function of depletion for different values of the critical slip displacement D_c. Stage 1 through 4 are indicated for D_c= 0.05 m (green line). The insert shows that the red line represents more brittle behaviour than the green line.*

Right: the Relative Slip Displacement (RSD) as function of True-Vertical depth for different depletion levels associated with the green curve on the left-hand side. A slip patch is defined by length of the fault (along dip) over which slip displacement occurs.

Uenishi & Rice (2003) showed that the slope of the slip-weakening branch in Figure 4 determines the length of the slip patch that need to be reached in order to cause instable equilibrium. That is: a steeper descending branch requires a smaller part of the fault to slip to become unstable. A steep descending branch is also referred to as brittle fault behaviour, whereas a slowly descending branch is referred to as a ductile fault behaviour. The critical slip length found in the 2D FE model is about 80% of Uenishi's analytically estimated length (Buijze et al., 2015).

Stage 3: Earthquake characterized by instable, seismic fault slip

Instable, seismic fault slip in Stage 3 is characterised by an acceleration of the rock mass adjacent to the fault and a rapid extension of the slip patch. This is demonstrated in Figure 6 for the case represented by the green line in Figure 5. The length of the slip patch at t=0 s (yellow line in Figure 6) corresponds with the length of the slip patch after 17 MPa depletion in Figure 5, and increase to more than 250 m after about 0.8 second. In the same period, the kinetic energy, which is representative for the mass velocity in the model, increases to about 0.4 MJ/m after 0.4 s before dropping to about 0.25 MJ/M after 0.8 s. At this point, the fault rupture process has come to an end and mass velocity waves are traveling to surface with constant kinetic energy (under the assumptions of this model).

The formation strain energy (purple line) and formation pressure energy (blue line) are delivering the energy for the rupture process: both are negative and attain a constant negative value after 0.8 s. Most of the energy released by the formation is dissipated by fault slip (green line), while the kinetic energy takes less than 1% in this particular case. The latter is referred to as the seismic efficiency.

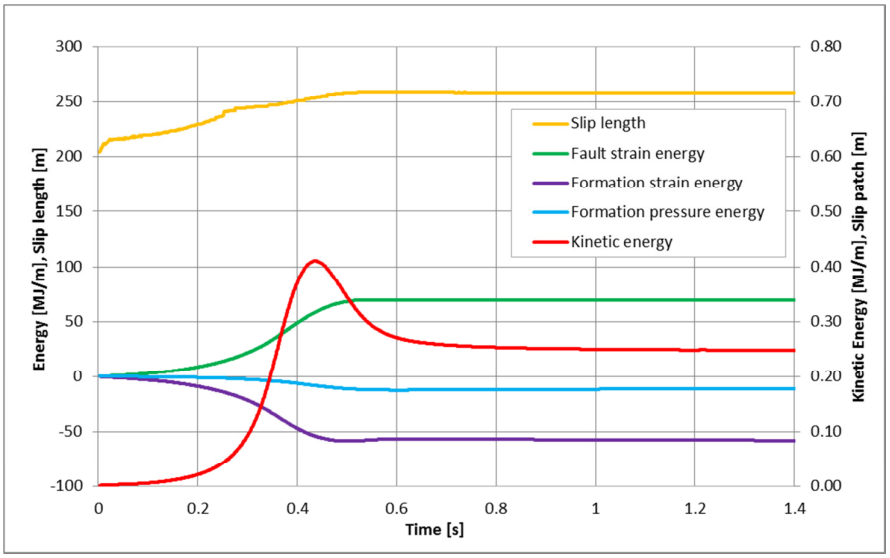

Figure 6 *The development of the slip patch (yellow line) during the rupture process (stage 3) for the green case in Figure 4.. The reservoir formation adjacent to the rupturing fault releases energy (formation strain energy, purple line, and formation pressure energy, blue line, are negative), which is largely dissipate by fault slip (green line). A small portion, less than 1% in this case, is kinetic energy that is radiated to surface and experienced as an earthquake.*

The length of the slip patch is constraint to the reservoir interval as shown in Figure 5. The green dashed arrow represents the additional length of the slip patch that is developed during the earthquake (in Stage 3). The slip patch length for the two other cases in Figure 5 also remain limited to the reservoir interval. However, as indicated by the yellow and red dashed arrows in Figure 5, the additional slip length during the rupture process in Stage 3 is larger for smaller critical slip displacement D_c. Consequently, the amount of kinetic energy that is radiating to surface is also larger, and so is the magnitude of the earthquake.

Meaning of the results

The following hypothesis can be formulated based on the insight that the slope of the descending branch of the fault slip behaviour determines the critical slip length at which a fault becomes instable

- No earthquake occurs along faults for which the critical slip length is larger than the length of the fault over the reservoir interval.
- The magnitude of an earthquake is related to the length of the fault over the reservoir interval minus the critical slip length.
- Earthquakes are less likely and have a smaller magnitude in parts of the field with smaller reservoir thickness (assuming the same brittle slip behaviour).

Furthermore, these results suggest that

- Stable fault slip (Stage 2) takes place (long) before an earthquake occurs, and that
- many faults may have developed a slip patch size close to the critical slip length at this moment in time

Some of the points are not new, but can now be related to geomechanical modelling parameters that are relevant to the occurrence of instable, seismic fault slip.

Concluding remarks

The geomechanical fault stability studies do not provide direct answers to questions related to which production scenario is better to reduce the frequency or magnitude of seismicity in the Groningen field. But one could ask the question: how can the current insight help to start formulating an answer? For instance:

- Are faults in an area with a higher seismic event rate closer to a critical state than faults in an area with a lower event rate? If so, this would imply that the current length of the slip patch is closer to their critical limit, and that minimal disturbance locally could cause an earthquake.
- Are earthquakes larger in magnitude in areas with larger reservoir thickness? Or larger along faults with more along dip exposure to depleting reservoir?

The geomechanical studies demonstrate that the local stress condition in the vicinity of the fault is dominating the slip and rupture process, which can only occur if fault slip-weakening behaviour is assumed. The rupture process is robust for uncertainty of the stress condition, the fault strength and orientation, and other model parameters. The occurrence of an earthquake provides the proof that the associated fault exhibits slip-weakening behaviour and that the critical slip length is exceeded.

Reservoir pressure fluctuation on larger scales may influence the local fault stress conditions positively or negatively. Segall (1989) argued that (also) fault slip and seismic events may occur outside a depleting area, Figure 7. This is also valid for areas with relatively larger depletion pressure compared to areas with lower depletion pressure, and implies that pressure gradients across the

field may contribute to the stress condition locally at potentially critically stressed faults. However, pressure gradients in the Groningen field are expected to remain small due to the good reservoir permeability, and so are the stress gradients and impact on the local fault stress condition. Also, areas with reduced shear stress loading can be expected, which should reduce the risk of starting a instable, fault rupture process. So, the contribution of field-scale stress gradients on the stability of faults is expected to be very small compared to much steeper stress gradient introduced by formation offset.

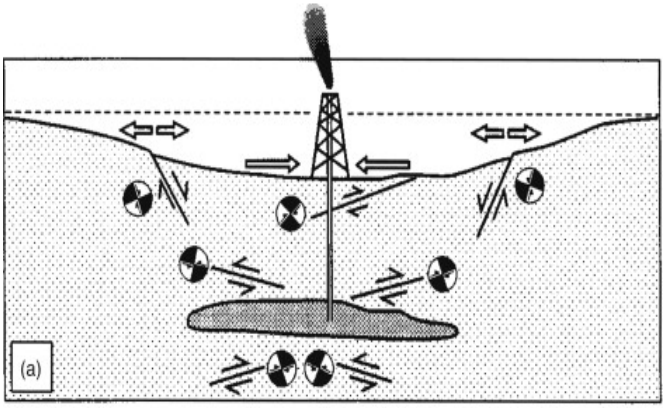

Figure 7 The principle of triggered seismicity outside a depleting reservoir (Segall, 1989).

As mentioned earlier, the difficulty in developing a predictive capability is the variability of the stress and strength condition locally, but also the availability of more and more accurate seismic event data in terms of location and magnitude is essential. The best opportunity is provided by the seismic event data captured by the two wells equipped with down-hole geophones. Using Full-Wave Inversion techniques, a more accurate fault location and magnitude determination is expected, including smaller events that are not (accurately) captured by the surface geophone array. Furthermore, statistical tools are being developed to verify the various hypotheses and find possible aerial differences that could be used to steer production scenarios.

References

Buijze, L., Orlic, B., Wassing, B.B.T. (2015), *Modelling fault rupture in a depleting gas field*. Report TNO project report 2015 R10844, November 2015.

Glab, M. and Van Eijs. R (2001), *Localisation of Sensitive Reservoir Settings for Induced Seismicity using FEM*, Report TNO-NITG 00-320-A

Mulders, F.M.M. (2003), *Modeling of stress development and fault slip in and around producing gas reservoirs*, Ph.D. thesis, Delft University of Technology

Orlic, B. and Wassing, B.B.T. (2012), *Modeling stress development and fault slip in producing hydrocarbon reservoirs overlain by rock salt caprocks*, ARMA 12-145, 46th US Rock Mechanics / Geomechanics Symposium, Chicago, Il, USA, 24-27 June 2012.

Roest, J.P.A., Kuilman, W. (1994), *Geomechanical analysis of small earthquakes at the Eleveld gas reservoir. SPE 28097, SPE/ISRM Rock Mechanics in Petroleum Eng. Conference, Delft, The Netherlands, 29-31 August 1994.*

Segall, P. (1989), *Earthquakes triggered by fluid extraction*. Geology, Vol. 17, pp.

Roest, J.P.A., Kuilman, W. (1994). *Geomechanical analysis of small earthquakes at the Eleveld gas reservoir. SPE 28097, SPE/ISRM Rock Mechanics in Petroleum Eng. Conference, Delft, The Netherlands, 29-31 August 1994.*

Uenishi, K., and J. R. Rice, (2003) *Universal nucleation length for slip-weakening rupture instability under nonuniform fault loading,* J. Geophys. Res., 108(B1), 2042, doi:10.1029/2001JB00168.

Van den Bogert, P.A.J. (2015), *Impact of various modelling options on the onset of fault slip and fault slip response using 2-dimensional Finite-Element Modelling*. Report SR.15.11455, Shell Global Solutions International B.V.

Visser, C. (edt.), *Groningen Field Review 2012, Static Modelling and Hydrocarbon Volume Determination,* Document number: EP201203204663

World Stress Map Project, http://dc-app3-14.gfz-potsdam.de/pub/introduction/introduction_frame.html

Zheng, Y. and Guises, R. (2014), *Dynamic Geomechanical Modelling to Assess and Minimize the Risk of Fault Slip during reservoir depletion of the Groningen Field – 1D Geomechanical Model*, Baker RDS NAM0001 Final Report.

Self-Organized Criticality

ExxonMobil Upstream Research Company
7 October 2015

Introduction

Groningen hazard assessments have understandably been based on well-established procedures in earthquake engineering that are widely applied to tectonic earthquake hazards. These assessments have been vetted by established experts providing a transparency to all stakeholders. Taking a longer-term perspective, research on induced seismicity including adaptation of new directions in tectonic hazard assessment and the statistics of emergent behavior may provide models with more predictive power. By considering attractive research opportunities now, a collaborative and interdisciplinary research program among key technical organizations can lead to an improved understanding of Groningen seismicity and more accurate hazard assessments. ExxonMobil, as a shareholder, is interested in supporting NAM as operator of the Groningen field in growing these collaborative relationships, particularly with TNO and SodM.

Statistical Mechanics of Earthquakes

Concepts from statistical mechanics have been adapted to a surprising range of disciplines such as finance, biology and cognition. One of these adaptations is applying phase transition theory to earthquake scaling behavior through the model of self-organized criticality (SOC). SOC was introduced in the 1980s as a simplified model of the scaling behavior seen in earthquake distributions. Early successes included deriving the universality of b=1 as the Gutenberg-Richter power-law exponent. Two schools of thought later emerged on whether SOC is a valid description of seismicity. These perspectives are well-described in an extended debate among seismology researchers in *Nature* in 1999. More recent work has found for example that the Southern California Earthquake Catalog is inconsistent with a key statistical characteristic of SOC (Yang, 2004).

A strength of SOC is the ability to derive power-law scaling behavior around the criticality point. Main (1995) applies this concept to derive magnitude frequency distributions above and below criticality, parametrized by a "tectonic temperature". The implementation challenge for this approach is calibrating this parameter to achieve a predictive model given the relatively small number of seismic events and the lack of a clear connection to depletion and production scenarios. Broadly speaking this challenge is emblematic of the school of thought that implementation of SOC concepts into a predictive model is difficult due to weak constraints on parameters.

Agent-based modeling is a newer approach to explore behavior of natural and engineering systems characterized by highly-interacting elements (Wilensky and Rand, 2015). Agent-based models relax the requirement of criticality that is central to SOC and so can explore a larger class of problems. They share a similar challenge to SOC of a difficulty developing predictive models. They are instead intended to develop process-level insights into complex systems. Looking at induced seismicity as a complex system emergent phenomenon presents the potential opportunity of leveraging agent-based methods to connect physical geomechanical models of reservoir depletion to statistical seismological models of earthquakes.

In summary, there is a large body of literature applying SOC to earthquakes, however its limitations as a predictive tool when constrained by limited data sets may restrict its use for earthquake modeling due to its limitations as a predictive tool. Recent work on emergent collective behavior lacking criticality or exploring connecting SOC techniques with other models and methods may provide a useful path forward but may also have similar limitations.

Summary

ExxonMobil is building a sustained and interdisciplinary induced seismicity research team. This team is focused on providing technical analysis of the Groningen seismicity issue in support of the operator, NAM. This is a challenging long-term problem that will benefit from diverse perspectives and collaboration. There are many attractive research opportunities that combine advancements in fundamental understanding with potential for direct application at Groningen and we are interested in pursuing collaborative relationships.

References

Ian Main, “Earthquakes as critical phenomena: Implications for Probabilistic Seismic Hazard Analysis”, Bull. Seismol. Soc. America 85(5),1299 (1995)

Uri Wilensky and William Rand, An Introduction to Agent-Based Modeling: Modeling Natural, Social, and Engineered Complex Systems with NetLogo, MIT Press, 2015.

Xiaosong Yang, Shuming Du, and Jin Ma, “Do earthquakes exhibit self-organized criticality?”, Physical Review Letters 92(22), (2004).

Various authors, “Is the reliable prediction of individual earthquakes a realistic scientific goal?”, Nature Debates (1999) http://www.nature.com/nature/debates/earthquake/